Greenhouse Gases: Science and Technology
Volume 8, Issue 3, June 2018, pp. 402-428.
DOI:10.1002/ghg.1767

Sulfur trioxide formation/emissions in coal-fired air- and oxy-fuel combustion processes: a review

Yerbol Sarbassov, Cranfield University, UK
Duan Lunbo, Southeast University, China
Vasilije Manovic, Cranfield University, UK
Edward J. Anthony, Cranfield University, UK

Correspondence to: Edward J. Anthony; Combustion and CCS Centre, Bedford MK43 0AL, Bedfordshire, UK. E-mail: b.j.anthony@cranfield.ac.uk

Abstract

In oxy-fuel combustion, fuel is burned using oxygen together with recycled flue gas which is needed to control the combustion temperature. This leads to higher concentrations of sulfur dioxide and sulfur trioxide in the recycled gas that can result in the formation of sulfuric acid and enhanced corrosion. Current experimental data on SO_3 formation, reaction mechanisms, and mathematical modelling have indicated significant differences in SO_3 formation between air- and oxy-fuel combustion for both the wet and dry flue gas recycle options. This paper provides an extensive review of sulfur trioxide formation in air- and oxy-fuel combustion environments, with an emphasis on coal-fired systems. The first part summarizes recent findings on oxy-fuel combustion experiments, as they affect sulfur trioxide formation. In the second part, the review focuses on sulfur trioxide formation mechanisms, and the influence of catalysis on sulfur trioxide formation. Finally, the current methods for measuring sulfur trioxide concentration are also reviewed along with the major difficulties associated with those measurements using data available from both bench- and pilot-scale units.

Keywords: Oxy-fuel combustion, sulfur dioxide, sulfur trioxide formation, catalysis

Table of Contents

1. Introduction

1.1 Oxy-fuel Combustion Technology

According to the International Energy Agency (IEA), 41% of the electricity generated in 2013 was produced from coal-fired power stations,[1] while data for 2015 indicated that about 45% of the anthropogenic CO_2 was produced from coal.[2] Current energy utilization trends indicate that energy generated from fossil fuels will continue to play an important role in the world energy portfolio in the foreseeable future. In this context, carbon capture and storage (CCS) has been proposed as a strategy to mitigate greenhouse gas emissions (GHG) from fossil fuel-fired power plants and industrial processes, and the Intergovernmental Panel on Climate Change (IPCC) suggests that CCS could potentially reduce CO_2 emissions from those systems by 80-90%.[3] CCS technology involves production of a highly concentrated CO_2 stream from a combustion process which can be transported to and stored in geological formations such as saline aquifers or depleted oil and gas reservoirs. Oxy-fuel combustion was initially proposed in 1982, to produce highly concentrated flue gas (CO_2) for enhanced oil recovery (EOR).[4,5] The concept was later explored by Argonne National Laboratory (ANL), where oxy-fuel tests were carried out at a pilot-scale facility.[6] In 1990, comprehensive work started on CCS concepts throughout Europe and the USA.[7,8] A simplified block diagram of oxy-fuel CCS systems is presented in Fig. 1, in which the most important feature of the process is that fuel is burned in a mixture of O_2 and CO_2 and steam from flue gas recycle (FGR) in order to moderate combustion temperatures to the same level as in an air-fired unit. As combustion occurs in the

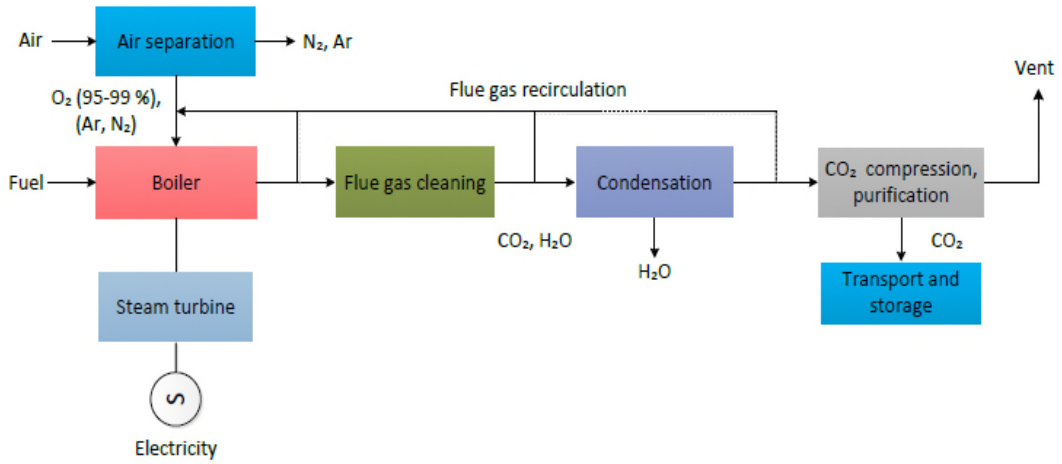

Figure 1 Principal scheme of oxy-fuel combustion process

effective absence of nitrogen, the flue gas consists mainly of CO_2 and steam, with impurities such as NO_x and SO_x. The composition of the concentrated CO_2 stream from oxy-fuel combustion was studied by Liu and Shao,[9] who found that N_2/Ar and O_2 concentrations typically varied from 1-6%, and 3-5%, respectively, depending on O_2 purity from the air separation unit (ASU) and the equivalence ratio. Also, the steam concentration in the flue gas was in the range of 10-40%, depending on the fuel properties and FGR.[9] Typical emissions from coal- and gas-fired power plants are reported by the IEA (Table 1).[10] Circulating fluidized bed combustion (CFBC) offer comparatively lower SO_2 and NO_x emissions, and in the case of pulverized coal (PC) technologies additional flue gas clean-up is required.

Table 1 Performance of coal- and natural gas-fired power plants

Plant (MW)	**Capacity factor (%)**	**CO_2 (g/kWh)**	**NO_x (mg/Nm^3)**	**SO_2 (mg/Nm^3)**	**PM[1] (mg/Nm^3)**	**Efficiency penalty (CCS) (%)**
PC-Ultra Super Critical (1050)[2]	80	740	<50 to 100 (by SCR)	<20 to 100 (by FGD)	<10	7 to 10 (post- and oxy-fuel combustion)
CFBC (460)[3]	80	880 to 900	<200	<50 to 100 (in situ)	<50	
PC A-Ultra Super Critical[4] <(1000)	-	669	<50 to 100 (by SCR)	<20 to 100 (by FGD)	<10	
IGCC (335)	70	669 to 740	<30	<20	<1	7
NGCC (410)	80	400	<20	Almost none	0	8

1. Particulate matter, 2. In operation (sliding pressure-type), 3. In operation (Poland), 4. Under development.

The flue gas passes through a cleaning process comprised of a series of steps, such as particle removal by an electrostatic precipitator (ESP), flue gas desulfurization (FGD) and selective catalytic reduction (SCR). The ESP system also prevents degradation of catalysts in the SCR unit. In addition, to avoid an accumulation of sulfur species in the SCR system, an FGD unit must be installed upstream of the SCR unit.[4] Studies to date suggest that due to O_2 separation, flue gas treatment and CO_2 compression, the net efficiency of oxy-fuel systems drops 7-11% points.[11–13] This increases the levelized cost of energy from such systems, which also significantly varies depending on the plant location, type of fuel and other assumptions used for evaluations.[11]

The purified CO_2 stream is then compressed and transported for geological storage.[14–19] Anheden et al.[15] reported that the SO_2 content in the CO_2 stream must be <200 mg/Nm^3, or even as low <50 mg/Nm^3, depending on CO_2 storage site requirements. Markewitz et al.[18] recommended that SO_x concentrations for CO_2 transportation should be kept below 100 ppm in order to reduce corrosion issues.[19] Also, SO_2 in the CO_2 stream may cause problems due to sulfation of calcium-containing minerals and formation of sulfates which decrease the permeability and may affect the storage capacity of the reservoir. In addition, nearly complete dehydration of the CO_2 stream is strongly desirable in order to inhibit corrosion,[20,21] and removal of various other impurities is necessary since they negatively affect all stages in the CCS chain.[22,23]

Typical contents of impurities in CCS systems are shown in Table 2, specifically for three oxygen-purity scenarios for oxy-fuel technologies, resulting in 85.0%, 98.0 and 99.9% CO_2 in the flue gas stream, respectively.[24,25] It can be seen that SO_2 and SO_3 concentrations in the CO_2 streams are higher in oxy-fuel combustion than in the pre-combustion and post-combustion schemes. White et al.[26] have highlighted that the SO_2 and SO_3 compounds can be removed from the CO_2 stream during the compression stage in the form of H_2SO_4 and that additional purification of the raw CO_2 stream is not required.

As stated above, sulfur species derived from coal-fired power plants are a major issue. Sulfur removal by limestone has been found to be an effective option to control SO_x emissions due to low capital and operational costs.[27,28] However, this option is not practical for PC boilers due to higher flame temperatures causing thermal decomposition of sulfation products ($CaSO_4$).[27,28] Recently, impacts of sulfur in oxy-fired PC boilers have been reviewed by Stanger et al.[29], and they noted that the formation of SO_3 is a major issue in coal-fired combustion boilers. However, there is less research on this issue for oxy-fuel combustion in fluidized bed combustion (FBC) boilers despite the fact that increased SO_2 and SO_3 concentrations are expected due to FGR and more pronounced corrosion issues on downstream surfaces are expected due to lower gas flow rates through the furnace.[30,31] This paper aims to provide a major overview of the subject of SO_3 formation and its emissions from air and oxy-fired boilers, given that at this time no such review exists.

1.2 Influence of Sulfur in Combustion Systems

The sulfur content in coal may vary from 0.2 to 11%, depending on the location and rank.[32,33] However, the values fall generally between 0.3 and 4.3%.[34] Typically, sulfur in coal is

classified as organic and inorganic.[32,35] The amount of organic sulfur is typically approximately one-half to one-third of the total.[35,36] Most organic and pyritic sulfur in coal is converted to SO_2 during combustion and only a small fraction of the sulfur is retained in the ash.[27] For example, studies for North Dakota coals showed 83 to 93% sulfur conversion to SO_2, depending on sulfur content and forms of sulphur in coal.[37] Similarly, 91% of sulfur conversion for a US eastern bituminous coal was observed by Croiset and Thambimuthu.[38] German lignite was also investigated in a pilot-scale 100 kW oxy-PC unit at Chalmers University and showed 67% conversion.[39] During combustion, part of the sulfur is retained in the fly ash by reacting with alkaline and alkaline earth metal compounds such as calcium carbonates, and sodium chloride.[40] Sulfur retention by the alkaline compounds is typically roughly 10 to 15%.[37,40] It has been reported that the sulfur retention in PC boilers and fluidized beds are different mainly due to different combustion temperatures.[41] Inorganic constituents of several Australian low-rank coals and ash characteristics (after combustion in a laboratory-scale fluidized bed) were investigated and it was noted that combustion of coals with high sulfur and sodium contents resulted in formation of low-melting-point compounds such as alkali sulfates in the ash, which are deposited as a coating on bed material surfaces.[42] This process can also cause bed material to become sticky and enhance ash build-up in the reactor. Coals with low sulfur and sodium content permit operation over a much longer time without any agglomeration and de-fluidization.[42]

Table 2 Composition of CO_2 streams for storage

Species	Pre-combustion		Post-combustion			Oxy-fuel		
	Selexol	Rectisol	Purity Low	Purity Med.	Purity High	Purity Low	Purity Med.	Purity High
CO_2 (vol%)	97.95	99.7	99.93	99.92	99.81	85.00	98.00	99.94
O_2 (vol%)			0.015	0.015	0.03	4.70	0.67	0.01
N_2 (vol%)	0.90	0.21	0.045[1]	0.045[1]	0.09[1]	5.80	0.71	0.01
Ar (vol%)	0.03	0.15				4.47	0.59	0.01
H_2O (ppm)	600	10	100	100	600	100	100	100
NO_x (ppm)			20	20	20	100	100	100
SO_2 (ppm)			10[2]	10[2]	20[2]	50	50	50
SO_3 (ppm)						20	20	20
CO (ppm)	400	400	10	10	20	50	50	50
H_2S+COS (ppm)	100	100						

[1]Total concentration of N_2 and Ar; [2]Total concentrations of SO_2 and SO_3

The main challenge with burning sulfur-containing coals is corrosion, which has been extensively studied in the case of conventional,[32,33,40] and more recently, in oxy-fuel combustion systems.[29] Most of the corrosion mechanisms associated with sulfur in air-combustion are well explored and apply equally well to oxy-combustion. Corrosion is caused by low-temperature-melting alkali salt deposits when burning coals rich in sulfur, chlorine and sodium compounds.[43] Longer operation of the units can lead to damage of heat exchangers by loss of metal or formation of cracks in high-temperature zones.[44] The presence of pyrite in coal is the main reason for the formation of clinkers when high-sulfur coals rich in pyrites (FeS_2) were burned.[43] Under such conditions, iron species occurring in high-sulfur coals act as fluxing agents, and enhance the melting of quartz and clays in the coal.[43] In addition, elevated levels of SO_3 in the molten salt result in an increase in solubility of the oxide scale on the metal.[45,46]

1.3 SO_3 Emissions in Combustion Systems

Formation of SO_3 is undesirable in combustion processes as it enhances low-temperature corrosion and formation of aerosol emissions.[30] By its nature, SO_3 is very reactive and converts easily to sulfuric acid in the presence of water vapour.[35] Formation of SO_3 is thermodynamically favoured at lower temperatures; however, cooling rates in practical systems retard the SO_3/SO_2 conversion rate. Moser[47] reported that the deposition of H_2SO_4 on downstream surfaces can be avoided by increasing the outlet temperature of the flue gas. Doing so, for example, by increasing the flue gas temperature in the air heater by 1.7ºC can result in an improvement of nearly 1% in the unit heat rate.[47] The annual benefit derived from the removal of SO_3 and the consequential reduction of corrosion downstream can exceed $500,000 for a 500 MW unit.[47] During combustion, most sulfur in fuel is oxidised to SO_2, while a limited amount of SO_2 may be converted to SO_3.[30,34,35,38] In addition, 0.5 to 1.5 wt % of SO_2 present in the flue gas may further oxidize to SO_3.[48] The SO_2-to-SO_3 conversion is dependent on several parameters such as: combustion temperature, O_2 concentration and the presence of catalytic compounds in the fly ash.[49,50] Tan et al.[51] have stated that the oxidation of SO_2 to SO_3 in typical PC boilers may reach 5%, depending on the sulfur content of the coal. Data from the UK power plants shown in Table 3[52] indicate the effect of excess O_2 concentrations on the formation of SO_3. It can be seen that operation under low O_2 concentration in the flue gas leads to significantly lower levels of SO_3.

SCR technology in coal-fired power plants can cause further oxidation of SO_2 to SO_3.[30,47] According to Moser,[47] this SO_2 oxidation to SO_3 in SCR can vary from 0.3% to 2%. Slightly lower values for bituminous coals (0.25-0.5%) compared to that of for sub-bituminous coals

(0.75 to 1.25%) were noted by Srivastava et al.[30] A more detailed study on SO_2 oxidation over honeycomb SCR catalysts was presented by Svachula et al.[53] According to these authors, the oxidation degree of SO_2 in SCR depends on several factors such as the vanadium content of the fuel and presence of other catalysts.[53] In addition, the reaction rate was found to be independent of oxygen and steam concentrations, but strongly inhibited by ammonia, and slightly enhanced by NO_x.[53]

Table 3 SO_3 formation at high and low oxygen concentrations

Power plant	O_2 %	SO_3 (ppm)	T_{DP}, (°C)[1]
Marchwood	3.0	20	130-160
	0.5	2-7	116-124
Poole	4.0	45	160
	<0.6	5	82
S.Denes	1.7	N/a[2]	>130
	>1.7	N/a	130
Ince	4.5	18	N/a
	1.0	7	N/a

[1]T_{DP} - dew point; [2]N/a - not available.

In wet FGD, sulfuric acid in the flue gas is rapidly cooled by liquid spray. Under these conditions, the sulfuric acid vapour undergoes a shock condensation process which leads to the formation of fine sulfuric acid aerosol particles.[54] According to Peterson and Jones,[54] aerosol droplets have a mean diameter of 0.1 to 1.0 μm, which makes the droplets effective at scattering visible light and can lead to a visible plume.[54] However, only a small percentage of the SO_3 will end up as sulfuric acid aerosols,[47] while part of it will condense on fly ash particles and be removed in the ESP or air preheaters. The quantity of fly ash, its surface area and alkalinity have a large impact on these processes.[47] The quantity of SO_3 removed by this mechanism is approximately 20% to 50% depending on the temperature and fly ash composition.[47] On the other hand, some studies on capturing suspended particulate matter from coal-fired plants showed that the presence of SO_3 in flue gas can be somewhat beneficial for effective operation of the ESP. Among such chemicals used to improve ESP performance, SO_3 is often used as a conditioning agent to reduce fly ash resistivity.[55,56]

In summary, FGR, FGD, the catalytic effect of fly ash and other pollutants can all increase the formation of SO_3 in the back end of the boiler. Relatively few studies on SO_3 emissions in oxy-fuel combustion are available in the literature. Thus, this paper reviews studies on SO_3 emissions in conventional air- and oxy-fuel combustion environments.

1.4 Objectives and Scope of the Paper

This paper aims to provide an extensive review on SO_3 emissions from coal firing in conventional air- and oxy-combustion environments. The available experimental data on SO_3 formation, uncatalyzed and catalyzed reactions, catalysis and the effect of combustion parameters are discussed. A brief introduction to oxy-fuel combustion, conversion of fuel sulfur to SO_2, and SO_3 emissions levels during the combustion are presented. Other issues such as effect of FGR, SO_2 emissions, effect of temperature and residence time, the catalytic effect of fly ash and available modelling studies are also outlined. In addition, this review includes an assessment of the existing analytical methods for measuring SO_3 concentrations in flue gases. Special attention is given to the experimental work conducted in laboratory-scale reactors to compare SO_2 to SO_3 conversion in air and oxy-fuel environments. Finally, the most recent investigations of SO_3 emissions from pilot- and industrial-scale experiments are also summarized.

2. Oxy-Fuel Combustion Environment

2.1 Flue Gas Recirculation

The amount of recycled flue gas used in the oxy-fuel systems should be sufficient to ensure flame temperatures similar to those under air-combustion conditions and comparable temperature profiles through the boiler.[5] In order to reach a similar adiabatic flame temperature as that in air-combustion, O_2 concentrations in the oxidant stream should be about 30%.[13,57] Typically, this requires two-thirds of the flue gas to be recycled, and an optimum FGR ratio lies between 0.6 and 0.8.[4,20,58,59] The recycle rate is defined as the amount of FGR per mole of fuel:[57]

$$\text{FGR rate} = v\left(\frac{\lambda_{\text{FGR}}}{[O_2]_{\text{Oxidant}}} - \frac{\lambda_{\text{FGR}}}{[O_2]_{\text{Asu}}}\right) \quad (1)$$

where v is the stoichiometric coefficient of O_2 for fuel used and $[O_2]_{asu}$ and $[O_2]_{oxidant}$ are O_2 concentrations provided to the ASU and the boiler, respectively (Fig. 2[57]). Alternatively, this can be presented as the recycled flue gas ratio:

$$\text{FGR ratio} = \frac{\text{Mol of recycled flue gas stream}}{\text{Total mol of flue gas stream of boiler outlet}} \times 100\% \quad (2)$$

Various FGR schemes were proposed by Nakayama et al.[60] In their studies, the difference between dry and wet flue gas recycle is due to the presence or absence of a dehydration (condenser) unit in the system flow (see Fig. 1). The wet FGR is extracted before the flue gas condenser.[61] Dry FGR can be extracted after passing through the condenser where restrictions on the moisture and SO_2 content exist.[61] An ASPEN-plus model developed by ANL indicates that SO_2 concentration builds up with increase of FGR fraction (Table 4[62]).

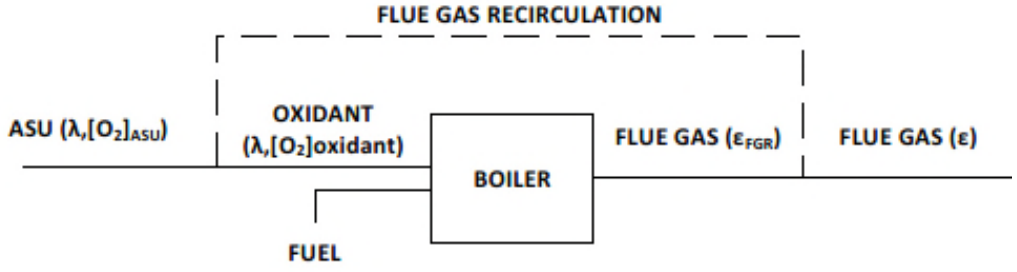

Figure 2 Simplified flue gas recycling scheme in oxy-fuel combustion

Wet FGR can be employed after passing through the FGD unit if the SO_2 concentration in the flue gas exceeds 3000 ppm.[63] FGR can be separated into primary and secondary streams. This makes it advantageous to utilize low-reactivity bituminous coals. The primary stream should be scrubbed, dried and cooled to a temperature of around 250ºC before entering the feeding mills.[4,63] Primary recycling is also used for coal transportation and removing moisture.[59,64] Thus, the removal of water-soluble acid gases such as SO_3 and HCl reduce the risks of corrosion.[57,63] Around 20% of the flue gas is taken as primary recycle, whereas the majority of the gas stream is extracted as the secondary stream.[4,16] The recycled flue gas temperature is determined mainly by the technical parameters of the recirculation duct, fan dimensions and ESP.[59] Therefore, the temperature of the FGR should be maintained between 200 and 300°C.[59,61,65] Operation of the hot recirculation fan at higher flue gas temperatures can lead to higher maintenance costs.[59]

2.2 SO_2 Emissions

Table 4 Effect of flue gas recycling on SO_2 concentration in the flue gas, based on 1000 ppmv without recycle.

FGR fraction	Sulfur concentration in the flue gas (ppmv)
0	1000
0.1	1080
0.2	1230
0.3	1390
0.4	1650
0.5	1920
0.6	2370
0.7	3110

In oxy-fuel combustion, the SO_2 concentrations are several times higher than that in conventional air combustion. However, in terms of the specific emissions (mg/MJ), SO_2 emissions are lower in the case of oxy-combustion.[38,66] As discussed by Dhungel et al.[67] and Fleig et al.[68] lower specific emissions can be explained by higher SO_2 retention by ash, and removal of SO_2 by condensate in the case of dry FGR. According to Liu and Shao,[9] SO_2 concentrations in oxy-fuel combustion can be 6 times higher than in an identical air-combustion unit. Higher concentration of SO_2 in the flue gas occurs due to the change in volumetric flow through the combustion furnace and FGR.[58] Tan et al.[51] have concluded that SO_2 concentrations in the furnace were 3-4 times higher than in air combustion for east US bituminous coals. Similar SO_2 concentrations were noted by Fleig et al.[39] in an oxy-PC unit. Relatively lower concentrations of SO_2 were measured by Duan et al.[69] in a 50-kW oxy-CFB. However, the SO_2 concentrations presented in this study were still higher than those seen in air-combustion. Croiset and Thambimuthu[38] have also

found that SO_2 levels with RFG tests doubled when compared to once-through tests in a 210 kW test unit. The authors observed a decreasing trend of S-to-SO_2 conversion from 91% in the air-fired case to 74% in O_2/CO_2 atmosphere. In FGR tests, this conversion was 64%. According to Croiset and Thambimuthu,[38] a possible reason for lower conversion was the sulfur retention by ash. Sulfur retention was also noted in experimental tests in the Chalmers University's 100 kW unit.[39] Relatively low S-to-SO_2 conversions in this case were noted in oxy-fired tests (43%) and in air tests (67%).

At higher temperature zones, the formation of SO_2 can significantly affect flame behaviour,[70,71] which was more evident in the presence of CO as it is reported that SO_2 inhibits the CO burnout rate.[72,73] Investigation on a bench-scale natural gas-fired 26 kW burner showed a clear decreasing trend in terms of CO emissions when 100 ppm SO_2 was added under sub-stoichiometric conditions.[34] Sulfur species can also decrease the NO levels in post-flame regions.[74–76] This occurs due to the catalysis of oxygen atom recombination reactions by SO_2.[74] Typical mechanisms are described by Glarborg et al.: [77]

$$X + SO_2 + M \rightarrow XSO_2 + M \quad (3)$$

$$Y + XSO_2 \rightarrow XY + SO_2 \quad (4)$$

where X and Y may be H, O or OH radicals. It is reported that under fuel-lean combustion conditions, the inhibition is mainly governed by the recombination of O radicals involving SO_3,[34] while under fuel-rich or stoichiometric conditions the interaction of SO_2 with radicals is believed to be more complex.[78,79] The most important radical removal step under stoichiometric and reducing conditions is caused by the recombination of SO_2 with H to form HSO_2:[78]

$$SO_2 + H + M \leftrightarrow HSO_2 + M \quad (5)$$

The presence of SO_2 also has an inhibiting effect on moist CO oxidation in air-firing environments. The inhibition was more pronounced at high atomic O levels; however, the presence of NO in the system significantly reduced the SO_2 effect.[77] This work has been extended recently by Giménez-Lopez et al.[79] who explored this phenomenon experimentally under CO_2-rich atmosphere to simulate oxy-fuel conditions. An important inhibition effect was evident in a CO_2 atmosphere as compared to a N_2-rich environment. This was due to the competition between CO_2 and O_2 for H radicals that reduces the formation of chain carriers via the O_2+H chain branching reaction. Lower inhibition was seen when the stoichiometry shifted to oxidizing conditioning.

3. Background for SO_3 Formation in Combustion

3.1 Homogeneous Conversion of SO_2 to SO_3

Past studies by Cullis and Mulcahy[35] and Jorgensen et al.[80] noted that photochemical tests on direct oxidation have been used to measure SO_3. This direct homogeneous oxidation of SO_2 is written as:

$$SO_2 + O_2 \rightleftharpoons SO_3 + O \qquad + 161.9\,kJ/mol \qquad (6)$$

However, limited SO_3 formation via reaction (6) was observed at temperatures below 900°C. As noted by Cullis and Mulcahy,[35] while direct oxidation of SO_2 to SO_3 is rather limited, it can be produced in much larger amounts catalytically. In addition to that, two dominant reaction pathways are recognized for homogeneous SO_2 oxidation to SO_3. The primary oxidation is the direct reaction of SO_2 with O radicals that occurs in post-flame zones of the combustor:

$$SO_2 + O\,(+M) \rightleftharpoons SO_3\,(+M) \qquad (7)$$

where, M represents a third body. Burdett et al.[81] investigated the rate of the direct oxidation reaction from 630 to 1080°C. The authors have tested SO_3 formation in $O_2/N_2/SO_2$ flow and proposed the following kinetic equation to predict formation of SO_3:[81]

$$\frac{d[SO]_3}{dt} = \frac{k_1}{RT}[SO_2][O_2] = \frac{A[SO_2][O_2]}{RT} e^{(-B/T)} \qquad (8)$$

where k_1=A exp(-B/T), A=2.6 (± 1.3) * 10^{12} mol^{-1} cm^3 s^{-1}, B=23000 ± 1200 K. $[SO_2]$, $[O_2]$ and $[SO_3]$ are partial pressures of respective gases. More detailed data on the kinetics of reactions (6) and (7) can be found elsewhere.[82–86] The second pathway occurs under moist conditions, where oxidation of SO_2 is enhanced in the presence of steam that increases via O/H radical concentration:

$$SO_2 + OH\,(+M) \rightleftharpoons HOSO_2(+M) \qquad (9)$$

$$HOSO_2 + O_2 \rightleftharpoons SO_3 + HO_2 \qquad (10)$$

The first route is the main source of SO_3 at higher temperatures,[34] while the second route contributes to SO_3 formation during the cooling of flue gases.[34,80] Formation of SO_3 based on reactions (9) and (10) is thermodynamically favoured when exhaust gases undergo the cooling process. Production of SO_3 by reaction (10) is insignificant at temperatures of 730°C and above.[87]

The effect of SO_2 concentration on SO_3 formation under oxy-fuel conditions was measured by Duan et al.[88] at constant reactor temperature of 600°C (Fig. 3). As can be seen, an increasing trend of SO_3 concentration was noted with an increase of SO_2 concentration in the reactor. In contrast, the conversion rate decreased with increase of SO_2 concentration, which can be

attributed to a pseudo-first-order reaction mechanism. These results were consistent with observations of Belo et al.[89], Fleig et al.[90] and Wang et al.[91]

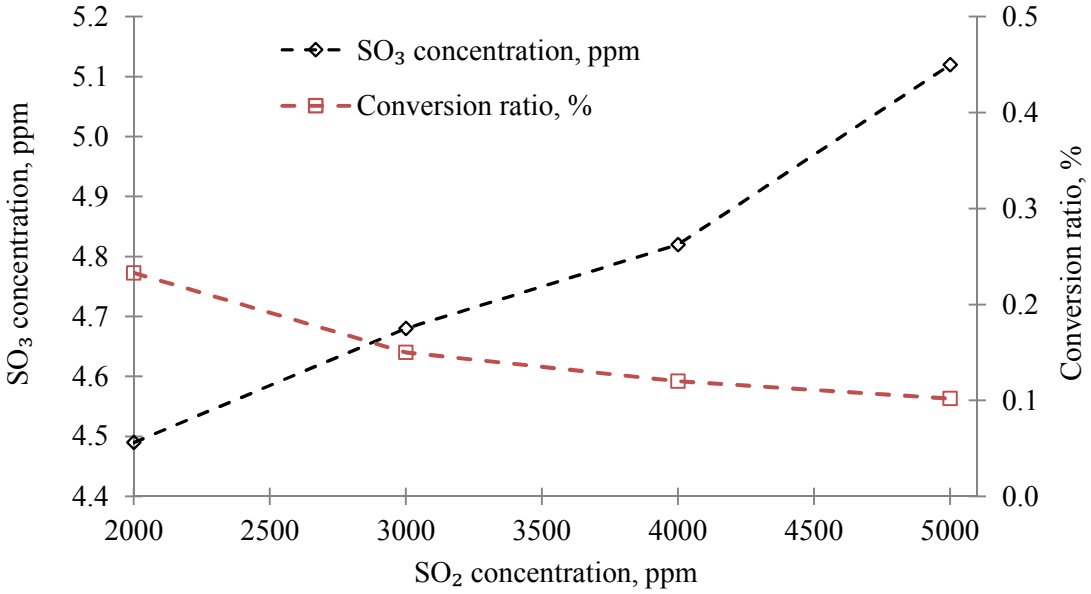

Figure 3 Effect of SO_2 concentration on homogeneous SO_3 formation under oxy-fuel condition. Test conditions: 6% O_2, 10% H_2O, CO_2 – balance, and 600°C (reactor temperature)

The SO_3/SO_2 thermodynamic equilibrium was plotted using data from the online calculator developed by Colorado State University.[92] Typical air- and oxy-fired flue gas compositions were selected with SO_2 levels of 1000 ppm for both air and oxy flue gases, Fig. 4. O_2 and H_2O concentrations were changed from air- to oxy-combustion conditions, while diluted N_2 was replaced by CO_2 to evaluate the SO_3/SO_2 equilibrium ratios at temperatures from 400 to 950°C. It can be seen in Fig.4 that the formation of SO_3 is thermodynamically favoured at lower temperatures, and for example, SO_3/SO_2 conversion was 100% at 400°C and 4.6% at 950°C. This equilibrium curve agrees with the results presented by Belo et al.[89] It is also interesting to point out that air- and oxy-flue gas composition showed similar results, and only small differences are noted in the range of 500-800°C.

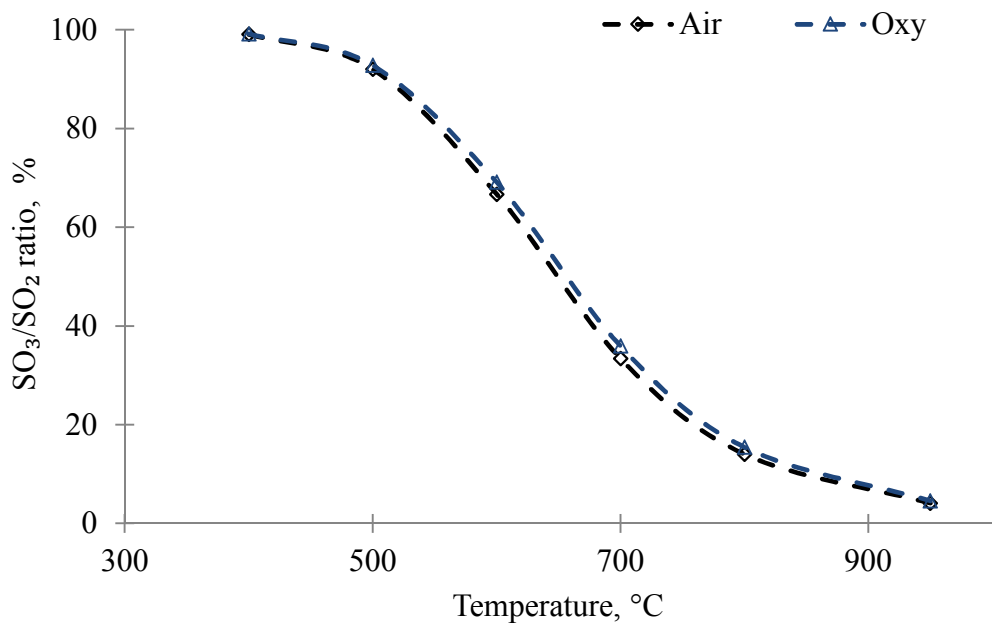

Figure 4 Thermodynamic SO_3/SO_2 equilibrium

Air-: SO_2-1000 ppm, O_2-4%, H_2O-6%, CO_2-15%, N_2-balance;
Oxy-: SO_2-1000 ppm, O_2-5%, H_2O-11%, CO_2-balance;

3.2 Catalytic Conversion of SO_2 to SO_3

There have been a number of investigations concerning the catalytic oxidation of SO_2 to SO_3.[93] Most of these investigations indicated higher conversion of SO_2 to SO_3 via heterogeneous catalysis[94–97] represented as:

$$SO_2 + O_2 \xrightarrow{\text{Catalyst } (Fe_3O_2, V_2O_5)} SO_3 + O \qquad (11)$$

Catalytic conversion of SO_2 to SO_3 by fly ash was investigated in a bench-scale reactor by Marier and Dibbs.[94] They concluded that the conversion of SO_2 to SO_3 was strongly enhanced due to the iron oxide in the fly ash whereas the reverse effect was noted in the presence of unburnt carbon in the fly ash.[94] Also, similar and supporting results were produced by Zhang et al.[95] Extended experiments on sulfation of CaO and MgO mixed with iron oxide indicated direct relation to the catalytic conversion of SO_2 to SO_3.[94] Similar work on the kinetics of SO_3 adsorption by CaO and MgO was undertaken by Thibault et al.[98] However, a subsequent study suggested that this might be due to the difference in grain size and porosity of the solid material.[98] A modelling approach called density functional theory (DFT) was applied by Galloway et al.[99] to explore binding mechanisms of SO_3 to other metal compounds. Compounds such as CaO, MgO, Na_2O and K_2O that are typically found in fly ash were included

in the model. The authors observed that SO_3 binds strongly with alkali and alkaline metals, with the effect being more pronounced with alkali metals (i.e., Mg<Ca<Na<K) through the formation of a sulfate (SO_4^{2-}).[99] Cao et al.[100] outlined two main interactions of fly ash with SO_3 based on temperature. First, fly ash could serve as an SO_3 adsorbent under low temperatures typical for the bottom section of boilers. At a temperature lower than the dew point of SO_3, it converts SO_3 to H_2SO_4 mist droplets in the presence of water. Subsequently, these droplets condense on fly ash surfaces. The pore structure of the fly ash, which is associated with the carbon residue, is responsible for condensation or adsorption of SO_3. Chang[101] investigated infrared adsorption of SO_2 on γ-alumina (γ-Al_2O_3) outlining two main factors, the number of hydroxyl groups and the temperature of the catalyst. Infrared spectroscopy showed that SO_2 is adsorbed on γ-Al_2O_3 in the form of sulfite species. SO_2 could also be oxidized on γ-Al_2O_3 to form aluminium sulfate. Vanadium catalyst contains a mixture of metal compounds of vanadium and alkali metal dispersed on a silica-based support. SO_2 to SO_3 oxidation by vanadium catalysts has been widely studied for SCR technology.[97]

3.3 SO_3 Sampling Methods

A number of different approaches for SO_3 measurement have been mentioned in the literature such as: the controlled condensation method (CCM), SO_3 monitor, isopropanol bottle method (IPA) and acid dew point measurements (DPM). These methods were examined by Jaworowski and Mack[102] who noted the limitations of each method in terms of reproducibility and accuracy. More recently, SO_3 measurements have been revised by Fleig et al.[103] Based on studies of Jaworowski and Mack[102] and Fleig et al.[103], a summary of each SO_3 measurement method is given below.

3.3.1 Controlled condensation method

CCM was classified as British Standard BS 1756-4:1977 and American Standard D-3226-73T, and has been the most widely used method for SO_3 measurements[102]. However, it should be noted that both of these standards have been withdrawn.[104,105] The principle of CCM is based on cooling flue gas to a temperature between the acid dew point and water dew point.

SO_3 is condensed in the quartz filter as well as on the glass walls of the sampling train as shown in Fig. 5. A sampling time of 30 minutes is required with a flow rate of 10 dm^3/min.[106] After gas sampling, a known quantity of distilled deionized water is used to flush out the filter and condenser to collect the H_2SO_4, which is then determined by the titration method using 0.005M barium perchlorate. As shown in Fig. 5, the quartz filter is used to capture particulates before entering the condenser and impingers. The probe and quartz filter should be maintained at 260°C to avoid the formation of aerosol particles and condensation of sulfuric acid.[106,107] The filtration of particulates from the sampling gas is crucial as the interaction of ash particles and SO_3 in the sampling train can lead to both positive and negative errors.[107]

The glass condenser should be maintained at 80 to 90°C. According to Maddalone et al.[107] CCM in laboratory tests collected 95% of H_2SO_4 with a variation coefficient of ±6.7%,[107] but the same authors indicated lower accuracy for the field tests. During the sampling, SO_2 reacts with water and dissociates into bisulfite and sulfite ions (reactions 12 and 13). The oxidation of SO2 in reaction (14) depends on the concentration of sulfite ions in the solution, which makes the reaction strongly pH-dependent (Fig 6):

$$SO_2 + H_2O \rightarrow H^+ + HSO_3^- \quad (12)$$

$$HSO_3^- \rightarrow H^+ + SO_3^{2-} \quad (1)$$

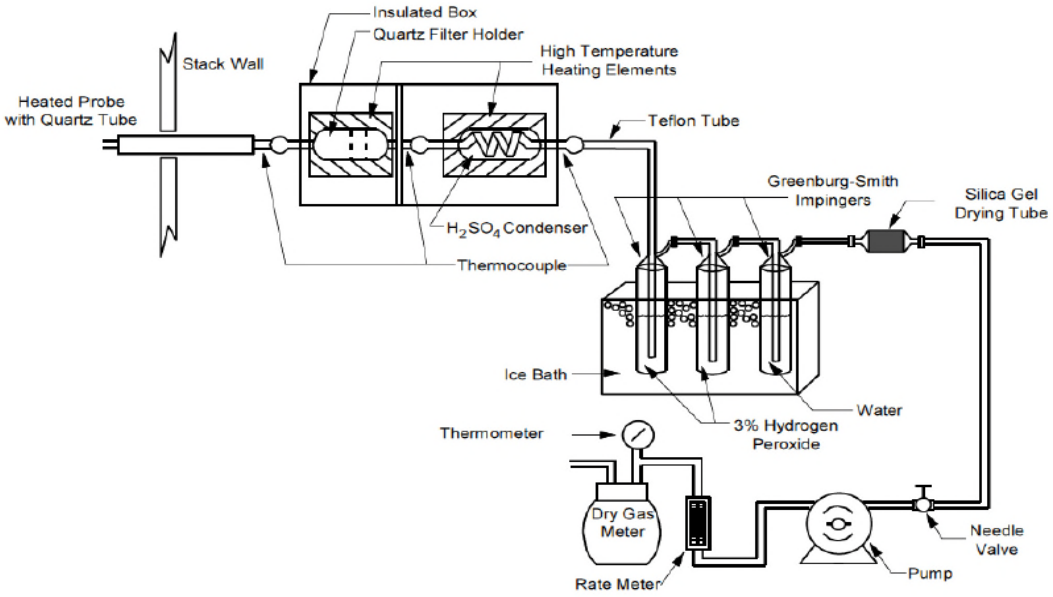

Figure 5 The modified controlled condensation method (CCM) SO_3 sampling scheme. [106]

$$SO_3^{2-} + \frac{1}{2} O_2 \rightarrow SO_4^{2-} \quad (14)$$

Figure 6 shows the calculated mole fraction of sulfur species as a function of pH at 25ºC in aqueous solution. It can be seen that sulfites dominate in alkaline solution while bisulfite dominates in acid solutions with a pH range of 3-7.[108] It is commonly accepted that at normal sampling conditions, the impinger solution must be slightly acidic, preventing sulfite formation and subsequent oxidation.[108] Therefore, purging of impingers with air is recommended to remove SO_2.

3.3.2 Isopropanol absorption bottle method

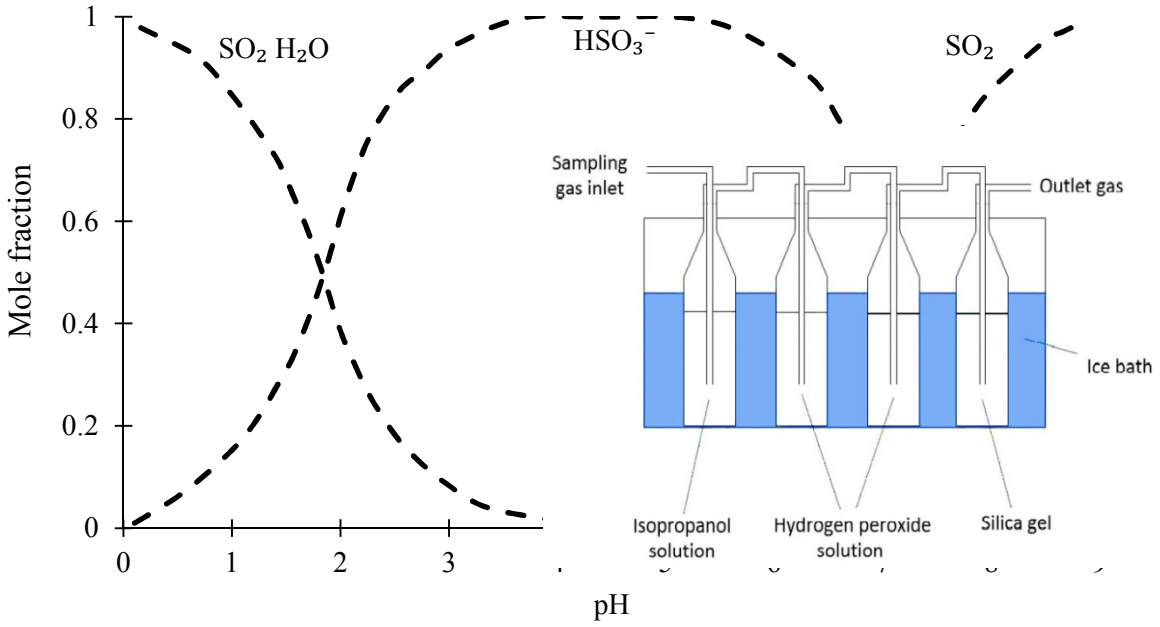

Figure 6 Effect of pH on the relative concentrations of the SO_2 species in solution [108]

This method is based on EPA Method 8

with some modifications. A schematic illustration of the isopropanol absorption method is shown in Fig. 7. The extracted flue gas is first cooled down as in the CCM by a glass condenser and passed through four bottles, which are kept in an ice bath. The first bottle is filled with 10 mL of 80% isopropanol solution diluted in water, the following two bottles are filled with 3% hydrogen peroxide solution, and the fourth bottle is used to capture moisture from the gas sample with silica gel. According to Cooper,[109] the most common error occuring during the

sampling of SO_3 in this method is absorption and oxidation of SO_2. Similar limitations were mentioned by Fleig et al.[103] where large amounts of SO_2 were absorbed in the isopropanol solution and resulted in a positive bias.[103]

3.3.3 Salt and glass bead methods

The first description of the salt method was provided by Kelman in the early 1950s.[110] This was later applied to industrial plant by Cooper et al.[109] The advantages of this method as highlighted by the authors are: no interference from SO_2 and simplicity of sampling. Flue gas containing SO_2 and SO_3 passes through the dry layer of NaCl and the sulfur trioxide reacts with NaCl.[110] This method was applied to detect SO_3 concentration in a 100 kW rig at Chalmers University.[111] A schematic of the salt method is shown in Fig. 8,[111] where salt is fixed in the tube with glass wool.[109,112] With a decrease of the gas temperature to approximately 500°C, SO_3 starts to react with water vapour to form gaseous sulfuric acid,[103,111] which then reacts with NaCl to form Na_2SO_4 and $NaHSO_4$.[111] The reactions occurring during the salt method are given as:

$$SO_3(g) + H_2O(g) \rightarrow H_2SO_4(g) \quad (2)$$

$$NaCl(s) + H_2SO_4(g) \rightarrow NaHSO_4(s) + HCl\,(g) \quad (16)$$

$$2NaCl\,(s) + H_2SO_4(g) \rightarrow Na_2SO_4\,(s) + 2HCl\,(g) \quad (3)$$

$$NaHSO_4(s) + NaCl\,(s) \rightarrow Na_2SO_4(s) + HCl\,(g) \quad (4)$$

$$4NaCl\,(s) + 2SO_2(g) + 2H_2O\,(g) + O_2(g) \rightarrow 2Na_2SO_4(s) + 4HCl\,(g) \quad (19)$$

The last reaction is undesirable as it leads to a positive bias.[103] Sulfation of NaCl is a slow reaction and mainly depends on temperature and SO_2 concentration. Vainio et al.[111] have extended this method by testing other salts (KCl, K_2CO_3, and $CaCl_2$) along with NaCl. Tests with NaCl and KCl showed comparable results to the CCM. Less convincing results were observed with K_2CO_3 and $CaCl_2$.[111]

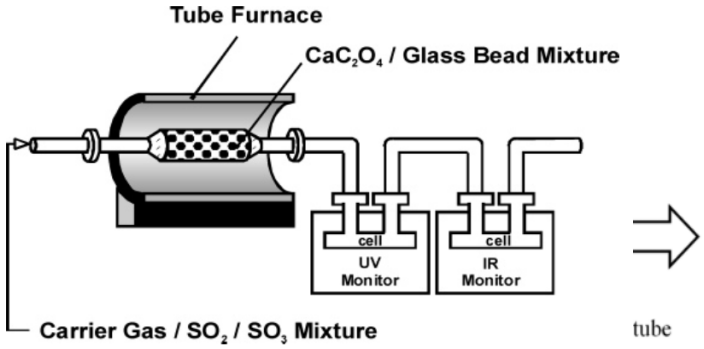

Figure 8 Salt tube preparation

Figure 9 Arrangement for SO_3 measurements by CaC_2O_4 [113]

3.3.4 Indirect measurements of SO_3

Ibanez et al.[113] described an indirect measurement method employing calcium oxalate, which is based on the next reaction:

$$SO_3 + CaC_2O_4 \rightarrow CaSO_4 + CO_2 + CO \quad (20)$$

This method is sensitive to temperature control and the reaction vessel should be maintained at 325°C. A mixture of gas passes through a plug of prepared CaC_2O_4 then through two optical cells in series (see Fig 9). The SO_2 content in the sample gas is monitored by means of UV spectrometry, while the SO_3 concentration is quantified indirectly measuring CO_2 in the second cell by IR spectrometry. The authors underlined that the preparation of reagent and calibration should be done very carefully to produce reliable results. A similar approach has been developed by Fateev and Clauson[114], but they presented only preliminary results.

Continuous SO_3 measurement by Fourier transform infrared (FTIR) and differential optical absorption spectroscopy (DOAS) was described by EPRI.[115] Subsequently a modified cross-duct probe design was developed to improve SO_3 measurements by FTIR. The result of continuous measurements for 3 days with FTIR was in good agreement with that determined by the CCM method. However, variation of SO_3 across probes was 10%.[31] An indirect test of SO_3 with FTIR has also been attempted by measuring HCl from reaction of NaCl with H_2SO_4. In this case, the exit gas temperature should be kept between 200-400ºC. However, at 200ºC, only about one-half the SO_3 was converted to HCl.[111] Chamberlain et al.[116] have also attempted to measure SO_3 concentrations with FTIR and the uncertainty of measurement was ±20 ppm. Given this range of uncertainty, the authors could not see a difference in SO_3 concentrations between air and oxy-fuel combustion. Therefore, both of these indirect methods still need to be improved before they can be reliably used in practice. Roy et al.[117] carried out such measurements for laboratory-scale oxy-fuel experiments, but they did not comment on the consistency of measurements and the effect of reaction conditions.

3.3.5 Pentol SO_3 monitor

This device was previously called the Severn Science reactive gas analyzer,[118] and Jackson et al.[118] were the first to describe this method and device. The principle of this instrument is that SO_3 and H_2SO_4 in the gas sample are absorbed as SO_4^{2-} in an aqueous solution of isopropanol. During the sampling, the solution is continuously passed through a bed of barium chloranilate where the following reaction occurs:

$$SO_4^{2-} + BaC_6O_4Cl_2 + H^+ \rightarrow BaSO_4 + HC_6O_4Cl_2^- \quad (21)$$

The released acid chloranilate ions absorb light at 535 nm, producing a purple-coloured solution, and the concentration of this chemical is continuously measured by a flow photometer. The amount of sulfate in the solution is proportional to the SO3 concentration entering the analyzer[119]. According to Dennis and Hayhurst[120], this instrument was slow to achieve steady-state performance and required moisture in the fluidization gases to ensure reliable readings. Cooper.[109] applied the Severn Science gas analyzer at the Orimulsion power plant, where the average results were 25% higher than those determined by the CCM approach. One reason for higher concentrations could be absorption of SO_2 in the isopropanol and partial oxidation of SO_3^{2-} to SO_4^{2-}. This was confirmed by peaks for both SO_3^{2-} and SO_4^{2-} in the ion chromatograph analysis.[109] The study by Fleig et al.[103] supports the reliability of this method, especially over longer continuous sampling periods. However, the average readings were still 20% lower compared to those from CCM.[103] Therefore, it is clear from the discussion above that there are still many issues related to accuracy of SO_3 measurements that need to be addressed.

3.3.6 Acid dew point measurements

The measurement of sulfuric acid dew point (ADP) temperature is one of the conventional ways to estimate the amount of SO_3 when H_2O concentration in the flue gas is known. Taylor[123] concluded that the condensation of sulfuric acid is a function of the surface temperature of the

Table 5 Sulfuric acid dew-point (ADP) correlations

Authors	Correlations
Verhoff and Banchero [121]	$\frac{1}{T_{Dew}+273.15} = 0.002276 - 0.00002943 \ln p_{H_2O} - 0.0000858 \ln p_{H_2SO_4} + 0.00000620 (\ln p_{H_2SO_4})(\ln p_{H_2O})$
Okkes [122]	$T_{Dew} = 203.25 + 27.6 \log p_{H_2O} + 10.86 \log p_{SO_3} + 1.06(\log p_{SO_3} + 8)^{2.19}$
ZareNezhad [122]	$T_{Dew} = 150 + 11.664 \ln(p_{SO_3}) + 8.1328 \ln(p_{H_2O}) - 0.383226 \ln(p_{SO_3}) \ln(p_{H_2O})$

sampling tube and the water vapour content in the flue gases. Measurements of ADP were conducted using a cooled electrical conductivity probe to determine the temperature where

condensation occurs.[124] The probe has two electrodes and a thermocouple. The ADP is identified by a sudden increase in the conductivity between electrodes on the surfaces due to the condensed liquid sulfuric acid solution. Currently, advanced portable devices (Lancom 200) are available to measure ADP of the flue gases.[124] The ADP changes with the moisture content of the flue gases, which is particularly important for an oxy-fuel combustion environment. Available correlations to estimate the ADP temperature are illustrated in Table 5. According to Verhoff and Banchero,[121] two methods have been developed to define the vapour and liquid equilibrium for aqueous sulfuric acid solutions. The first method was determined by measuring the vapour-liquid compositions and temperature at equilibrium. The second method takes into account liquid and pure components to estimate the equilibrium vapour and liquid compositions via thermodynamics. Based on these two methods, Verhoff and Banchero[121] have proposed a correlation to predict the dew point of sulfuric acid. More recently, ZareNezhad[122] has proposed a new correlation to predict flue gas sulfuric acid. Based on these correlations, Stanger et al.[29] compared both correlations for composition of flue gas derived from oxy-fuel combustion. The authors concluded that the Verhoff and Banchero method over-estimate experimental dew points at low SO_3 concentrations and high moisture content. The Okkes correlation has been found to be better suited for flue gases with moisture content higher than 25%.[29]

4. Influence of Oxy-fuel Parameters on SO_3

4.1 Effect of O_2/CO_2 Environment

SO_3 concentrations in an oxy-fuel environment are several times higher than in a typical air-combustion environment.[38,125] Higher SO_3 and SO_2 concentrations along with wet FGR will result in a higher ADP temperature, which leads to corrosion issues. At the bench-scale level, the formation of SO_3 in an O_2/CO_2 environment was investigated by several researchers, for example by Fleig et al.[90,126] Sporl et al.[127] Belo et al.[128] and more recently by Duan et al.[88] According to these authors, elevated O_2 concentration in oxy-fuel combustion enhances SO_3 formation. Belo et al.[89] have observed that O_2 concentrations of 3%, 5% and 10% resulted in SO_2 oxidation of 3-10%. These results agree well with the equilibrium calculation of Zheng and Furimsky.[129] Fleig et al.[90,126] concluded that replacing N_2 with CO_2 had a strong effect at higher temperatures. This might be due to higher effectiveness of third-body collisions, the effect of which is smaller at lower temperatures.[88] Fleig et al.[90] also noted 30% higher SO_3 concentrations when the CO_2 environment was compared to that of N_2. A sensitivity analysis

at 1027°C indicated that SO_3 formation was enhanced due to the increase of concentrations of radicals due to the third-body (M) reactions:

$$HO_2\ (+\ M\ )\ \rightleftharpoons\ H + O_2\ (+\ M) \quad (22)$$

$$H + O_2 \rightleftharpoons\ O + OH \quad (23)$$

The formation of H radicals is enhanced via reaction (22), and they then react with O_2 to form OH radicals according reaction (23). In addition, FGR increases the level of impurities such as NOx, SO_2 and CO that are believed to enhance the SO_3 formation to some extent as discussed below.

4.1.1 Effect of NO_x emissions

It has been noted that NO_x may have a catalytic effect on SO_2/SO_3 conversion even at low temperatures.[35,130,131] This effect can occur through either a direct or an indirect route by interaction with the radical pool composition.[34] At low temperatures SO_2 may react directly with NO_2 to produce SO_3:[130]

$$2NO\ +\ O_2 \rightleftharpoons\ 2NO_2 \quad (24)$$

$$NO_2\ +\ SO_2 \rightleftharpoons\ NO\ +\ SO_3 \quad (5)$$

According to Wendth and Sternling[131] the SO_2 oxidation was second order in respect to NO and had low activation energy at high concentrations of NO, and the reaction is of the first order in respect to NO with high activation energy at low concentrations of NO. At low concentrations of NO, reaction (24) is slow, and SO_2 oxidation can occur via the following route:[131]

$$NO\ +\ O_2 \rightleftharpoons\ NO_3 \quad (6)$$

$$NO_3\ +\ SO_2 \rightleftharpoons\ SO_3 + NO_2 \quad (27)$$

In addition, at low temperatures NO may indirectly increase SO_3 formation by converting HO_2 in reactions (9) and (10) back to OH radicals:[34]

$$NO + HO_2 \rightleftharpoons NO_2 + OH \quad (28)$$

This was noted by Fleig et al.[126] when a small amount of NO (100 ppm) favoured the formation of SO_3. The authors also noted an increase in SO_3 concentrations when more OH radicals were available through reaction (28) at temperatures higher than 1027°C and SO_3 was formed through reactions (9) and (10).[126] They also reported a notable increase in SO_3 formation in the presence of 50 ppm NO in an oxy-fuel environment.

$$H + O_2(+\ M) \rightleftharpoons HO_2(+\ M) \quad (7)$$

According to Glarborg et al.,[34] the rate of reaction (29) is higher in a CO_2 environment than in N_2 which favours HO_2 formation. Excess formation of OH via reaction (28) promotes

secondary formation of SO_3 via reactions. This effect was more pronounced in a CO_2 environment.[126] In the extended numerical work by Fleig et al.[126] a higher value for the third-body coefficient of 2.5 for CO_2 (instead of 1.0) resulted in negligible (2%) reduction of SO_3, which is still higher than that in the air-firing case. Thus, the impact of SO_2 oxidation by nitrogen oxide during cooling is likely to be small and the effect of NO can be assumed to be negligible in oxy-fuel combustion.[131]

4.1.2 Effect of carbon monoxide

Previous studies showed that the CO concentration in oxy-fuel is higher than that in air combustion processes due to relatively higher flame temperatures,[129,132,133] and most CO is formed in or near the burner region.[133,134] In high-temperature zones in a CO_2-rich environment, the thermal dissociation of CO_2 can also contribute to higher CO concentrations:[134]

$$CO_2\ (+M)\ \rightleftharpoons CO + O\ (+M) \qquad (30)$$

However, this reaction occurs only at temperatures significantly higher than 930°C.[134] CO_2 can compete with O_2 for atomic hydrogen, and will lead to the formation of CO:[132,134]

$$CO_2\ + H \rightleftharpoons CO + OH \qquad (31)$$

Simultaneously, during the formation of CO in the flame zone, the recombination of CO with OH can take place[85] and this will increase the formation of H radicals due to reverse reaction (31). This will compete with reaction (9) for OH radicals and that reduces the formation of SO_3 as noted in the experiments of Wang et al.[91] and Fleig et al.[90] It is worth mentioning that an early experiment from the staged combustion of a CH_4/H_2S/air mixture showed enhanced SO_3 formation in the presence of 1100 ppm of CO.[85] The maximum SO_2 oxidation took place at flame temperatures between 1300 and 1650°C for single and staged combustion. A narrow temperature range of 1100 to 1300°C was observed for the test where the secondary air supply was delayed for 30 ms. These authors postulated that the maximum SO_3 formation was only a transient phenomenon. The SO_3 concentration changed as the reactions continued in the downstream gas. In addition, there was no enhancement of SO_3 for residence time beyond 90 ms. The authors believe that enhancement of SO_3 formation was dependent on the air/fuel ratio of each combustion stage and the delay interval between the first and second stage[85]. These results were also supported by Bayless et al.[135] In the experimental work of Fleig et al.[90] addition of 1000 ppm CO into the system increased the SO_3 formation significantly compared to the test without CO addition. The measured SO_3 concentrations were three times higher at a temperature of 927°C with 3% O_2. However, a further increase of CO to 3000 ppm showed

only a small difference compared to the 1000 ppm CO addition. In summary, it appears that the maximum SO_3 formation in the presence of CO takes place at temperatures between 827 and 1027°C. Lower formation of SO_3 at temperatures higher than 1127°C was noted by Fleig et al.[90] This indicates that SO_3 formation is significantly affected by the temperature where burnout of the fuel takes place. In general, these results agree well with the studies of Merryman and Levy.[85]

4.1.3 Effect of steam

The wet FGR in oxy-fuel combustion can increase the steam level to 25-35% in the combustion system.[136] This increase may enhance secondary formation of SO_3 via $HOSO_2$ reactions (9) and (10). In the tests by Fleig et al.[90] a more pronounced effect of steam on SO_3 formation was noticed between 1130 and 1200°C. In the presence of steam OH radicals can be formed by the reaction of H_2O with O radicals:[84]

$$H_2O + O \rightleftharpoons OH + OH \quad (32)$$

and also by the decomposition of steam as noted by Wine et al.:[137]

$$H_2O \rightleftharpoons OH + H \quad (8)$$

Decomposition of HO_2 and OH release through reactions (22) and (23) shifts reaction (34) to the left and enhances SO_3 formation. In addition, the third-body efficiency of H_2O is higher than that of CO_2 and N_2.[90] Fleig et al.[90] have pointed out that an increase of H_2O from 0.1% to 1.1% and 8.7% result in higher SO_3 concentrations at temperatures between 927 and 1127°C. At 1174°C and 8.7% H_2O, SO_3 concentration reached 23 ppm. However, in the presence of combustibles, the inhibiting effect of steam in SO_3 formation was noted.[90] This observation agrees well with the previous conclusion of Glarborg et al.[77] A less pronounced effect of H_2O on SO_3 was noted by Belo et al.[128] The effect of steam was also studied by Duan et al.[88] at 600°C, who identified an increase of SO_3 concentration from 3.7 ppm to 7.1 ppm when steam increased from 5% to 15%.

In contrast to these studies, a decreasing SO_3 formation was observed in homogeneous tests of Wang et al.[91] In this work, higher concentrations of steam (15 to 35%) were employed to simulate wet FGR. The authors claimed that less pronounced formation of SO_3 was due to the inhibiting effect of steam. In oxy-fuel combustion tests, a further increase of H_2O to 35% showed a stronger inhibiting effect on SO_3, which is consistent with the result from Fleig et al.[90]

According to Hindyarti et al.[138] and Glarborg et al.[77], major consumption of SO_3 in combustion could be due to reactions (34) to (36).

$$SO_3 + H \rightleftharpoons SO_2 + OH \quad (34)$$

$$SO_3 + O \rightleftharpoons SO_2 + O_2 \quad (35)$$

$$SO_3 + OH \rightleftharpoons SO_2 + OH_2 \quad (36)$$

In addition, in their experiments H_2O concentrations were higher than SO_2 concentrations, and under such conditions, steam was more likely to compete for O radicals. As a result, O radicals formed OH radicals resulting in lower SO_3 formation through reaction (7).

4.2 Temperature and Residence Time

Flint and Lindsay[139] and Burdett et al.[81] carried out pioneering investigations on oxidation of SO_2 in quartz tube reactors in air environment. In both tests an increasing trend in homogeneous SO_3 formation with temperature and residence time was noted. Increase of SO_3 formation with increase of furnace and flame temperatures was also investigated earlier by Crumley and Fletcher[140] (Table 6). Later, a similar approach in an O_2/N_2 environment was explored by Belo et al. [89] As shown in Table 6, the homogeneous conversion ratio from 0.04% to 0.77% was achieved by increasing temperature from 400 to 1000°C. In their test, a conversion increase was noted when the reaction temperature went above 700°C, but temperatures above 900°C were required for significant conversion for the tests with a residence time of 1 s.[89] For that residence time, the maximum conversion was 0.36%, which agrees well with the previous results of Flint and Lindsay[139] and Burdett et al.[81] The SO_2 to SO_3 conversion vs temperature is illustrated in Fig 10. More results on homogeneous SO_3 formation in quartz tube reactors can be found in Table 6.

The effect of temperature on homogeneous SO_3 formation under different environments was also studied by Duan et al.[88] In their studies SO_3 concentration increased with temperature even at the lower temperature range (400 to 700°C).[88] The reason for SO_3 formation in this experiment could be the high SO_2 concentration (3000 ppm) employed. It is known that at lower temperatures SO_3 is formed by oxidation of molecular oxygen via reactions (9) and (10) and that SO_3 formation is thermodynamically favoured with decreasing temperature. Overall, the observations of Duan et al.[88] agree with the findings of Belo et al.[128] Fleig et al.[90] have carried out experiments on homogeneous SO_3 formation over a much wider temperature range (Table 6), and they concluded that less than 1 ppm SO_3 was formed at temperatures below 727°C. The lower level of SO_3 seen in their work was due to the short residence time, as noted by Flint and Lindsay[139] and the low level of H_2O (1.11%).

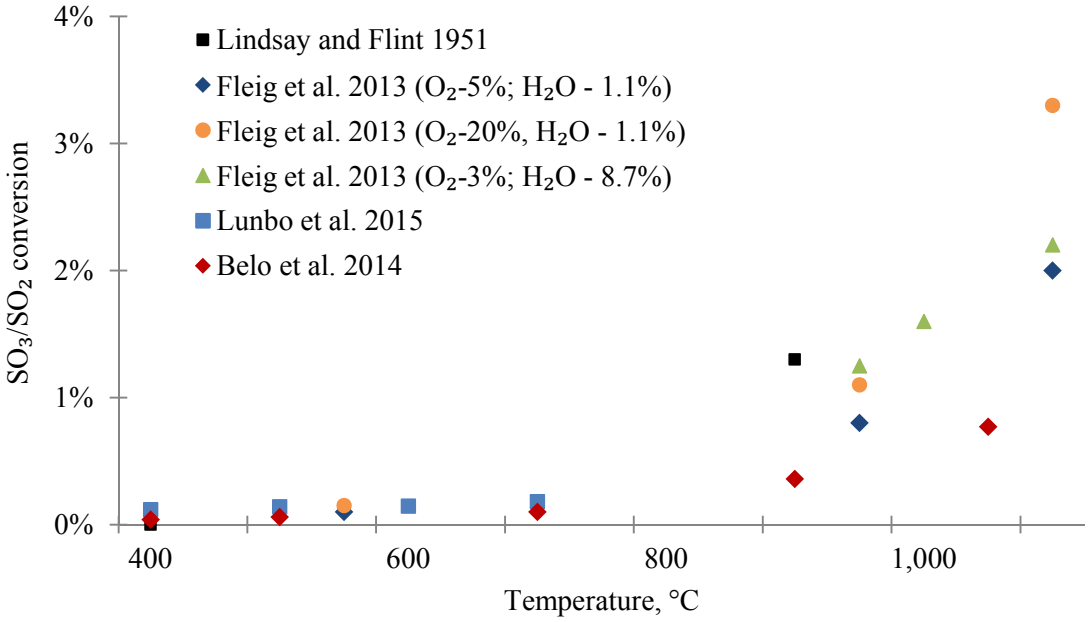

Lindsay and Flint, 1951; SO_2-1400 ppm, O_2-21%, H_2O-8%, Balance-N_2, res.t-4.3 s;
Fleig et al. 2013; SO_2-1000 ppm, O_2-5/20%, H_2O-1.1/8.7%, Balance-N_2, res.t-5 s;
Duan et al. 2015; SO_2-3000 ppm, O_2-5%, H_2O-6%, Balance-N_2, res.t-1.5 s;
Belo et al. 2014; SO_2-1000 ppm, O_2-5%, H_2O-3%, Balance-N_2, res.t-1 s;

Figure 10 Effect of reactor temperature on homogeneous formation of SO_3

Table 6 Homogeneous SO_3 formation in quartz tube flow reactors

Reference	Reactor Size (d x l) mm	Temperature (°C)	Inlet gas composition	Flow rate (L/min)	Residence time (s)	Maximum temperature (°C)	$SO_3/(SO_2+SO_3)$ (%)
Barret et al.[141]	25.4 x 610	1030-1530	Air + 0.7% SO_2	3.4	5.5-5.7	1530	0.2
Flint and Lindsay[139]	14 x 1829	500-900	Air (+ H_2O-8%), SO_2(1400 ppm)	1.7-8.5	0.9-9.6	900	0.36 - 4.8
Burdett et al.[81]	10 x 450	850-1066	SO_2(0-5500 ppm); O_2 (0-21%); bal-N_2	0.5-5	Up to 6	960	0.36
Belo et al.[89]	12 x 250	400-1000	Gas mixture (SO_2-1000 ppm, H_2O-3%, O_2-5%, bal-N_2)	0.5-1.5	0.3-0.9	1000	0.14 – 0.77
Fleig et al.[90]	50 x 900	527-1400	SO_2-1000 ppm, O_2-3%, H_2O-1.11%, bal-N_2/CO_2,	1.0	Up to 5	1400	0.1-1.7
Duan et al.[88]	15.5 x 1115 (420)[1]	400-700	O_2-6%, SO_2 -3000 ppm, H_2O, bal-N_2/CO_2,	3.7	1.5	700	0.1–1.5
Wang et al.[91]	50 x 1500	350-1050	O_2-5%, SO_2 –500, 1500, 2500 ppm, H_2O-0.03%, bal-CO_2,	2.0	N/S[2]	950	0.11 0.16 0.21

[1] Only (420mm) of total length is heated; [2] N/S-Not specified. Based on size of tube and flow rate, calculation shows long residence time for this work

4.3 Catalytic Effect of Fly Ash

Metal oxides such as Fe_2O_3, Al_2O_3 or CuO can act as a catalyst in SO_2 oxidation, while alkali and earth metal oxides such as MgO and CaO can adsorb SO_3.[94] The catalytic effect of fly ash on SO_3 formation in oxy conditions was investigated by Belo et al.[89] who found that: (i) the total conversion of SO_2 to SO_3 was only about 1.8%; (ii) the effect of Fe_2O_3 was the most pronounced; and (iii) fly ash samples produced under air- and oxy-fuel conditions showed no significant difference. Also, the SO_3 concentration increased to 17.8 ppm at 700°C in the presence of ash, while only 1 ppm was observed without ash.[89] A stronger catalytic effect at 400 and 500ºC was noted by Duan et al.[88] compared to the tests of Belo et al.[89] who noted more pronounced catalytic effect at 700°C. High CaO content in ash can significantly reduce SO_2 concentrations, as noted by Ahn et al.[125] in the pilot-scale tests with PRB coal (22.2% CaO in ash). By contrast, enhanced SO_3 formation was observed for an Illinois coal, which contains 1.9% CaO in the ash, and a high sulfur content, as shown in Tables 7 and 8.

Hence, it may be concluded that pronounced catalytic effects were observed in bench-scale tests rather than in the pilot-scale tests. However, large units could perform differently due to the heat transfer rates, inconsistency in fuel composition and loading requirements. Interestingly, the effect of Fe was not observed in the presence of combustibles in pilot-scale tests of IFK.[127] For this reason, detailed experiments with a wide range of coals are still required under oxy-fuel combustion conditions to evaluate both catalytic oxidation and absorption by fly ash.

Table 7 XRF analysis of ashes used for SO_3 tests in oxy-fuel tests

Ash analysis	Solid Fuel	SiO_2	Al_2O_3	Fe_2O_3	CaO	MgO	Na_2O	K_2O	TiO_2	P_2O_5	SO_3
Belo et al.[89]	A	52.9	34	7.13	1.41	0.98	0.158	0.518	2.16	0.275	0.24
	B	69	24.2	2.16	0.87	0.737	0.275	0.604	1.65	0.176	0.28
	C	53	26.5	8.34	4.66	1.667	0.979	1.058	1.13	1.508	0.97
Sporl et al.[127]	A	58.9	26.2	6.8	1.2	0.7	0.1	0.4	2.4	0.2	0.3
	B	64.4	21.5	1.2	0.4	0.7	02	0.4	3.9	0.0	7.2
	C	33.2	23.0	11.4	7.0	1.8	1.3	0.9	1.2	1.8	22.7
Couling et al.[142]	Williamson coal	50	20.5	15.9	5.18	1.14	0.68	2.41	1.05	0.1	4.78
Ahn et al.[125]	PRB coal	30.46	14.78	5.20	22.19	5.17	1.94	0.35	1.30	1.07	8.83
	Utah coal	60.89	14.52	5.09	6.11	1.39	1.41	0.57	0.88	0.59	2.33
	Illinois coal	49.28	17.66	14.57	1.87	0.98	1.51	2.26	0.85	0.11	2.22
Kenney et al.[143]	Sub-Bit coal	34.56	16.05	6.16	19.79	4.23	1.24	0.50	1.29	0.81	11.67
	Low-S Bit coal	56.30	30.78	5.58	0.84	0.82	0.23	2.67	1.78	0.15	0.71
	High-S Bit coal	50.85	20.53	15.56	3.52	0.96	1.02	2.11	0.94	0.52	2.81
	Lignite	41.99	13.96	6.47	14.84	4.50	1.56	1.93	0.54	0.18	11.99
Duan et al.[88]	Bituminous coal	45.12	34.14	4.16	8.66	1.36	0.462	0.99	1.53	0.09	3.06
	Bituminous coal	37.84	18.52	10.37	19.99	4.51	2.55	0.37	1.09	1.09	3.07
Wang et al.[91]	Lignite	64.39	18.04	3.42	4.68	1.27	0.90	0.93	0.48	0.95	4.69
	Bituminous coal	48.82	29.81	3.99	4.57	1.12	1.12	1.17	0.64	0.26	8.23
Jurado et al.[144]	Cerrejon coal	60.69	22.01	7.43	2.27	2.90	1.06	2.32	0.92	0.21	
	CCP-biomass	44.36	2.49	2.47	7.78	3.96	0.36	24.72	0.12	12.04	

4.4 SO_3 Emissions from Pilot-scale Studies

Ahn et al.[125] extensively studied SO_3 formation in 1.5 MW oxy-PC and 330 kW oxy-CFB combustor units. Three types of US coals were tested (PRB, Utah and Illinois), and the sulfur content is provided in Table 8. During the oxy-fuel test with Illinois coal (3.98% S) the SO_3 concentrations were 4 to 6 times higher at 530°C. However, similar SO_3 concentrations were observed for oxy- and air-combustion at higher temperatures (~930°C) in PC tests, and they were lower than those measured at 527°C, which suggests the secondary formation of SO_3 and the catalytic effect of metal oxides in pilot-scale tests. In oxy-CFB only Utah coal was tested, and the trend of SO_3 emissions was consistent with that of oxy-PC combustion. However, on a normalised base (mass per energy unit), no difference was found between oxy- and air-firing. SO_3 measurements were also undertaken at IFK in a 500 kW oxy-PC combustor.[145] In these tests, ESP was included along with SCR[145] and the SO_3 sampling was made from the inlets and outlets of ESP and SCR. Roughly 62% SO_3 capture was noted in the SCR unit. Higher SO_3 levels were noted in oxy-fuel runs and there was less influence of the SCR on the ADP.[146,147] Babcock-Hitachi tested SO_3 emissions in a 1.5 MWth oxy-fuel combustion facility which included SCR, clean energy recuperator (CER), FGR dry precipitator (DESP) and wet electrostatic precipitator (WESP).[148] Two different coals, with low sulfur, but high ash content, were used in this experimental campaign. SO_3 concentration at the DESP outlet was reduced to <1 ppm by decreasing the flue gas temperature to 90°C at the DESP inlet. Similar results were obtained for air- and oxy-fuel combustion. Most SO_3 was trapped in the CER unit.[148]

Little data exist in the literature on SO_3 formation from oxy-biomass or co-firing combustion. Some SO_3 measurements were performed by Jurado et al.[144] in a 100 kW oxy-PC unit during co-firing combustion tests. Cerrejon coal/cereal co-products were blended at levels of 50%/50% and 75%/25%. Wet FGR was employed in these tests with varied steam content. Overall SO_3 concentrations appear to show slight increases with an increase of biomass percentage in the mixture, which might be due to the higher content of alkali oxides (primarily K_2O) in biomass fly ash. Other SO_3 measurements at pilot- and industrial-scale combustors are summarized Table 8. With regard to SO_3 measurement techniques, the CCM method is most commonly used for pilot-scale tests.

Table 8 A detailed lists of SO_3 measurement campaigns under air- and oxy-fuel combustion

Authors	Type of fuel and sulfur content	Type of reactor	Measurement equipment	SO_3 measurement method	SO_3 (ppm)
Abele et al.[6]	Sub-bituminous (S-0.57%);			Controlled condensation method	Air-0.03; Oxy-0.76;
Tan et al.[51]	East-bituminous (S-0.95%); Sub-bituminous (S-0.22%); Lignite (S-0.6%);	0.3 MW_{th} Vertical combustor	Data acquisition: Honeywell Series S9000e controller; Gas analyzer	Not specified	Air-27 ng/J; Oxy-75 ng/J; Oxy-0.14 ng/J;
Ahn et al.[125]	PRB (S wt.%-0.23), Utah (S wt.%-0.53), Illinois (Swt.%-3.98)	1.5 MW PC combustor; 0.3 MW_{th} CFB	SO_2 Gas analyzer (CAI Model 601 NDIR) and FTIR (Nicolet Magna-IR 550) spectrometer	Controlled condensation method	PRB Air: below 5[13] Utah Air: 5[13] Utah Oxy: 5[13] Illinois Air: 31[13] Illinois Oxy: 117[13]
Eddings et al.[149]	Illinois coal pellets (S - 4.0%)	BFB reactor	FTIR	Controlled condensation method	Air: 12[13] Oxy: 10[13]
Kiga et al.[66,29]	Australian low sulfur coals with: A (S-0.45%); B (S-0.96%); C (S-0.38%);	1.2 MW IHI Aioi facility	Non-dispersive infra-red gas analyzer (HORIBA ENDA-1610), Gas chromatography (Shimadzu 14APFP);		Coal A: Air-2; Coal A: Oxy-7; Coal B: Air-9; Coal B: Oxy-9; Coal C: Air-3; Coal C: Oxy-11;
Fleig et al.[103]	Propane and SO_3 injected to unit;	100 kW Oxy-fired test unit combustor	Nondispersive infrared (NDIR) analyzers (NGA 2000 Fisher Rosemount); IC (ICS -90 DIONEX)	Controlled condensation method used as reference case to other methods: 1. Isopropanol absorption bottle method; 2. Salt method; 3. Pentol SO_3 monitor	CCM results: Air case: 34; Oxy-case 25[14]:9; Oxy-case 30[14]: 56; Oxy-case 35: 25

Authors	Type of fuel and sulfur content	Type of reactor	Measurement equipment	SO_3 measurement method	SO_3 (ppm)
Vainio et al.[111]	Mixture of gases: (SO_2, H_2O, O_2, N_2 and H_2SO_4)	Bench-scale horizontal tube reactor	ICS-90 Ion chromatography (DIONEX)	Salt method: four types of salts tested (NaCl, KCl, K_2CO_3, $CaCl_2$)	Salt method results: NaCl: Air – 30[1]; NaCl: Oxy – 46[1];
Spörl et al.[150]	Australian coals with sulfur: (A-0.3%; B-0.7%; C-0.7%)	20 kW combustion rig; L x D (2.5 x 0.2 m); Flow rate: 11.5 m^3/h	IC (DIN EN ISO 10304)	Controlled condensation method	Coal A: Air – 2; Oxy: 6 – 35[3]; Coal B: Air – 8; Oxy: 18 – 50; Coal C: Air – 1; Oxy: 2–30;
Monckert et al.[147]	Klein Kopje, Lausitz, Rhenish, Ensdorf coals (S-1%)	0.5 MW down-fired Oxy-PC	SEM-BSE, SEM-MAP	Controlled condensation method	Air: 8; Oxy: 85;
Roy et al.[117]	Victorian coals Loy Yang, Morvell and Yallourn (S- 0.5%)	10 kW oxy-fired BFB	Gas analyzer (MX6 iBrid) GC (Agilent GC 7890A);	Calcium oxalate with glass beads	Dry Oxy: 11 mg/MJ; Air: 15 mg/MJ; Dry Oxy-fuel 14 mg/MJ;
Duan et al.[88]	Fly ash, bituminous coal (S-0.5%)	50 kW oxy-CFB	Titration; IC DX-120 (DIONEX)	Controlled condensation method	Air-2, Oxy-8;
Wang et al.[91]	Lignite coal (S-0.6%); Bituminous coal (S-3.69%)	Oxy PC unit	ICS -90 DIONEX	Controlled condensation method	Oxy Bituminous coal: (500 to 3000 ppm SO_2); 13 to 105; Oxy Lignite: (500 to 3000 ppm SO_2); 0.5 to 80;
Hemis[31]	Illinois bituminous coal	Hoosier Energy' Merom Station	FTIR; IC (Desert Analytics);	FTIR and Controlled condensation method	Air tests: Day-1 FTIR-37.33 versus CCM-30.4; Day-2 FTIR-37.66 vs CCM-29.1;
Cao et al.[100]	Bituminous and subbituminous coals (S-3.5%);	Fixed bed reactor,	IC (DX-120);	Modified controlled condensation method	Air. Site1: Bituminous coal SCR inl-22; SCR out–24; Air preheater out–7; ESP in-6;

Authors	Type of fuel and sulfur content	Type of reactor	Measurement equipment	SO_3 measurement method	SO_3 (ppm)
	Three types of fly ashes	Full-scale utility boilers			FGD inl–7; FGD out–4; Site 2: SCR inl-23; SCR out-24; Air preheater out-21; ESP out-17; FGD inl-17.5; FGD out-15; Site 3: Sub-bituminous: below 2 at all locations
Kenney et al.[143]	LSB[4] (S-0.9%), HSB[5] (S-3.2%); Sub-bituminous (S-0.3 %), Dried lignite (S-0.7%);	Oxy-fired pilot plant 15 MW_{th}, Alstom;	N/A	SO_3 executed from four locations of boiler; Controlled condensation method.	Sub-bit Air: 0.5[1]; Oxy with SO_x control: 1.6[1]; LSB air: 28.8; oxy: 39.4; HSB air-41; Oxy-186.3; Lignite air-30; oxy-45.9;
Jurado et al.[144]	EI Cerrejon coal (S-0.58%); Cereal co-product (S-0.16%)	0.1 MW pulverized oxy-fuel combustor	FTIR, ESEM/EDX, XRD	Controlled condensation method	Air: EC-3.7; EC/CC (50/50%)-20.2; CC-25.4; Oxy: EC-20.6; EC/CC (50/50%)-35.9; EC/CC (75/25%)-16.8;
Davis[151]	USA Williamson coal (S-1.7%);	E.ON 1 MW Combustion Test Facility	XRF, SEM	SO_3 Monitor (Severn Science analyzer); Controlled condensation method	Not specified;
Dhungel et al.[67]	Medium Sulfur Bituminous Coal	Emission reduction test facility 0.16 MW oxy-fired system;	Dry sorbent injection; Gas analyzer	Controlled condensation method	Not specified; roughly 3 to 5 times higher in oxy-fuel
Stanger et al.[152]	Callide coal S-0.3	Callide oxy-fuel plant		Controlled condensation method	Air < 0.06; Oxy: 0.6-3.7;

[1] Average value is presented; 2. Oxy-25/30: 25% or 30% of O_2 in the oxidizer stream; [3] Range of SO_3 values is provided for this particular test as initial parameters were different; [4] LSB-low sulfur bituminious; [5] HSB- high sulfur bituminious;

4.5 Modelling Studies of SO_3 Formation

Only a few numerical studies on SO_3 formation are available in the open literature for oxy- as compared to air-combustion. Burdett et al.[81] simulated the effect of operating bed pressure on SO_2-to-SO_3 conversion for air-combustion. The predictions for bed pressure (600 kPa) and temperature of 900°C with 10% of O_2 in the flue gas clearly indicated increasing SO_3 formation with increasing oxygen formation. This work suggests that under such conditions the potential conversion of sulfur-in-fuel to SO_3 could be as high as 20%. Fleig et al.[126] modelled homogeneous gas-phase SO_3 formation for oxy-fuel combustion conditions with a model which is described by Giménez-Lopez et al.[79] and which was initially developed by Glarborg et al.[153] CHEMKIN-PRO was used to model homogeneous reactions considering plug flow reactor. More recently, Belo et al.[89] implemented a kinetic model of Burdett et al.[81] for residence time of 0.3 to 0.9 s (Table 6). Due to thermodynamic considerations, the maximum conversion of SO_2 to SO_3 was at low temperatures and further increases of temperature to 900 and 1000ºC decreased the SO_3 by ~6.8 and ~3.2%, respectively.[89] SO_3 formation was also modelled by Schneider and Bogdan,[154] for an oil-fired boiler.

5. Research Needs

A significant amount of effort has been made to evaluate SO_3 concentrations from laboratory-scale to commercial-scale units. However, oxy-fuel combustion requires more attention in terms of better understanding SO_3 formation mechanisms. At this point the majority of SO_3 measurements have been conducted in conventional PC and gas-fired combustion systems, while only a few studies are available for oxy-fired FB combustors and pilot-scale studies are still sparse. Major research should concentrate on the effect of FGR and catalytic conversion. SO_3 formation both depend on gases such as NO, CO and their effects may be different in oxy-fuel combustion and, hence more experiments are needed on SO_3 formation with different types of coals. Development of pressurized FBC systems would also require SO_3 formation tests as experimental data on the effect of pressure are rare.

In the case of analytical methods, all the current post-combustion SO_3 measurements still have technical challenges associated mainly with temperature control as SO_3 is a very

reactive molecule and SO_3 can easily be lost in the sampling line. At present, CCM is the most used and reliable technique to quantify SO_3 concentrations, while other methods such as the salt method or calcium oxalate with glass beads need to be improved.

6. Conclusions

The present paper reviews the formation SO_3 in coal combustion systems, and especially oxy-fuel technology. The following conclusions can be drawn:

- SO_3 concentration in oxy-fuel combustion is typically several times higher than that in air combustion. The higher level of SO_3 is mainly due to the increased concentrations of O_2, H_2O and SO_2 in the boiler
- Wet flue gas recycling is associated with higher SO_3 concentration than dry flue gas recycling. An increased amount of H_2O promotes SO_3 formation apparently due to the production of OH radicals. However, H_2O concentrations higher than 15% in the system strongly inhibit SO_3 formation. Inhibition appears to be more pronounced in actual PC tests than in simulated flue gas tests.
- Higher conversion of S to SO_3 occurs near the burnout region where O_2 is found in excess amounts. In this region, gas-phase homogeneous formation is dominant for SO_3 formation.
- The presence of gases such as NO and CO may enhance SO_3 formation. However, these effects appear to be small compared to other factors such as combustion temperature, excess O_2 and presence of catalysts.
- SO_3 formation is enhanced due to catalytic effect of fly ash. Higher concentrations of Fe_2O_3 and V_2O_5 and other metal oxides increase SO_3 concentrations significantly. Adsorption of SO_3 by alkali and alkaline earth metal oxides is also an important phenomenon.
- The CCM method appears to be the most dependable technique for measuring SO_3 concentrations.

Acknowledgements

The authors would like to thank Dr Nelia Jurado from Cranfield University (UK) and Dr Emil Vainio from Abo Akademi (Finland) for useful advice on the controlled-

condensation method (CCM) and the salt method, and also for providing valuable information. The financial support from Nazarbayev University under “Talap” studentship is also greatly acknowledged. This work was completed as part of a PhD program at Cranfield University for one of us (YS).

References

1. IEA, Tracking Clean Energy Progress 2016, Energy Technology Perspectives 2016 Excerpt IEA Input to the Clean Energy Ministerial, (2016).
2. IEA, CO_2 Emissions from fuel combustion, Highlights, (2017).
3. IPCC, *IPCC special report on carbon dioxide capture and storage*. Prepared by Working Group III of the Intergovernmental Panel on Climate Change, ed by Metz B, Davidson O, de Coninck HC, Loos M and Meyer LA. Cambridge University Press, Cambridge, United Kingdom and New York, NY, USA (2005).
4. Toftegaard MB, Brix J, Jensen PA, Glarborg P and Jensen AD, Oxy-fuel combustion of solid fuels. *Prog Energy Combust Sci* **36**(5):581-625 (2010).
5. Buhre BJP, Elliott LK, Sheng CD, Gupta RP and Wall TF, Oxy-fuel combustion technology for coal-fired power generation. *Prog Energy Combust Sci* **31**(4):283-307 (2005).
6. Abele AR, Kindt GS, Clark WD, Payne R and Chen SL. An experimental program to test the feasibility of obtaining normal performance from combustors using oxygen and recycled gas instead of air, Report ANL/CNSV-TM-204, Argonne National Laboratory, Argonne, (1987).
7. Edge P, Gharebaghi M, Irons R, Porter R, Porter RTJ, Pourkashanian M *et al.,* Combustion modelling opportunities and challenges for oxy-coal carbon capture technology. *Chem Eng Res Des* **89**:1470-1493 (2011).
8. Wall T, Liu Y, Spero C, Elliot L, Khare S, Rathnam R *et al.*, An overview on oxyfuel coal combustion—State of the art research and technology development. *Chem Eng Res Des* **87**(8):1003-1016 (2009).
9. Liu H, Shao Y. Predictions of the impurities in the CO_2 stream of an oxy-coal combustion plant. *Appl Energy* **87**(10):3162-3170 (2010).
10. IEA, Energy Technology Perspectives 2012; Pathways to a Clean Energy System. IEA, Paris, France (2012).
11. Davison J. Performance and costs of power plants with capture and storage of CO_2. *Energy* **32**(7):1163-1176 (2007).
12. Müller M, Schnell U, Grathwohl S, Maier J and Scheffknecht G, Evaluation of oxy-coal combustion modelling at semi-industrial scale. *Energy Procedia* **23**:197-206 (2012).
13. Wall TF. Combustion processes for carbon capture. *Proc Combust Inst* **31** (1):31-47 (2007).
14. Jordal K, Anheden M, Yan J and Strömberg L, Oxyfuel combustion for coal-fired power generation with CO_2 capture - Opportunities and challenges. In: *The 7th International Conference on Greenhouse Gas Control Technologies* (GHGT-7), September. Vancouver, Canada, (2004).
15. Anheden M, Rydberg S and Yan J, Consideration for removal of non-CO_2 components from CO_2 rich flue gas of oxy- fuel combustion. In: *IEA Oxyfuel Workshop*. (2008).

16. Dillon DJ, White V, Allam RJ, Wall RA and Gibbins J, Oxy-combustion processes for CO_2 capture from power plant. Mitsui Babcock Energy Limited, Engineering investigation report No. 2005/9, IEA greenhouse gas R&D programme (2005).
17. Gibbins J, Chalmers H. Carbon capture and storage. *Energy Policy* **36**(12):4317-4322 (2008).
18. Markewitz P, Kuckshinrichs W, Leitner W, Linssen J, Zapp P, Bongartz R *et al*., Worldwide innovations in the development of carbon capture technologies and the utilization of CO_2. *Energy Environ. Sci* **5**:7281-7305 (2012).
19. de Visser E, Hendriks C, Barrio M, Mölnvik MJ, de Koeijer G, Liljemark S *et al*., Dynamis CO_2 quality recommendations. *Int J Greenh Gas Control* **2**(4):474-484 (2008).
20. Andersson K, Johnsson F. Process evaluation of an 865 MWe lignite fired O_2/CO_2 power plant. *Energy Convers Manag* **47**(18-19):3487-3498 (2006).
21. Aspelund A, Jordal K. Gas conditioning-The interface between CO_2 capture and transport. *Int J Greenh Gas Control* **1**(3):343-354 (2007).
22. Burnol A, Thinon I, Ruffine L and Herri JM, Influence of impurities (nitrogen and methane) on the CO_2 storage capacity as sediment-hosted gas hydrates - Application in the area of the Celtic Sea and the Bay of Biscay. *Int J Greenh Gas Control* **35**:96-109 (2015).
23. Li H, Yan J, Yan J and Anheden M, Impurity impacts on the purification process in oxy-fuel combustion based CO_2 capture and storage system. *Appl Energy* **86**(2):202-213 (2009).
24. IEAGHG "Effects of Impurities on Geological Storage of CO_2", 2011/04, June, 2011 Available at: http://hub.globalccsinstitute.com/sites/default/files/publications/16876/effects-impurities-geological-storage-co2.pdf [Accessed 01 December 2017].
25. Talman S. Subsurface geochemical fate and effects of impurities contained in a CO_2 stream injected into a deep saline aquifer: What is known. *Int J Greenh Gas Control* **40**:267-291 (2015).
26. White V, Torrente-Murciano L, Sturgeon D and Chadwick D, Purification of oxyfuel-derived CO_2. *Int J Greenh Gas Control* **4**(2):137-142 (2010).
27. Cheng J, Zhou J, Liu J, Zhou J, Huang Z, Cao X *et al.,* Sulfur removal at high temperature during coal combustion in furnaces: a review. *Prog Energy Combust Sci* **29**(5):381-405 (2003).
28. Anthony EJ, Granatstein DL. Sulfation phenomena in fluidized bed combustion systems. *Prog Energy Combust Sci* **27**(2):215-236 (2001).
29. Stanger R, Wall T. Sulphur impacts during pulverised coal combustion in oxy-fuel technology for carbon capture and storage. *Prog Energy Combust Sci* **37**(1):69-88 (2011).

30. Srivastava RK, Miller CA, Erickson C and Jambhekar R, Emissions of sulfur trioxide from coal-fired power plants. *J air waste Manag Assoc* **54**:750-762 (2004).
31. *Continuous Measurement of SO_3 in a Coal-Fired Power Plant*. EPRI, Palo Alto, CA, 2006. 1010375.
32. Attar A. Chemistry, thermodynamics and kinetics of reactions of sulphur in coal-gas reactions: A review. *Fuel* **57**(4):201-212 (1978).
33. Raask E. Sulphate capture in ash and boiler deposits in relation to SO_2 emission. *Prog Energy Combust Sci* **8**(4):261-276 (1982).
34. Glarborg P. Hidden interactions-Trace species governing combustion and emissions. *Proc Combust Inst* **31**(1):77-98 (2007).
35. Cullis CF, Mulcahy MFR. The kinetics of combustion of gaseous sulphur compounds. *Combust Flame* **18**(2):225-292 (1972).
36. Glassman I, Yetter RA, *Combustion*, Fourth Edition. Academic press Elsevier. pp. 421-420 (2008).
37. Zygarlicke CJ, Stomberg AL, Folkedahl BC and Strege JR, Alkali influences on sulfur capture for North Dakota lignite combustion. *Fuel Process Technol* **87**(10):855-861 (2006).
38. Croiset E, Thambimuthu KV. NO_x and SO_2 emissions from O_2/CO_2 recycle coal combustion. *Fuel* **80**(14): 2117-2121 (2001).
39. Fleig D, Andersson K, Johnsson F and Leckner B, Conversion of sulfur during pulverized oxy-coal combustion. *Energy Fuels* **25**(2):647-655 (2011).
40. Cutler AJB, Raask E. External corrosion in coal-fired boilers: assessment from laboratory data. *Corros Sci* **21**(11):789-800 (1981).
41. Sheng C, Xu M, Zhang J and Xu Y, Comparison of sulphur retention by coal ash in different types of combustors. *Fuel Process Technol* **64**(1-3):1-11 (2000).
42. Vuthaluru HB, Zhang D and Linjewile TM, Behaviour of inorganic constituents and ash characteristics during fluidised-bed combustion of several Australian low-rank coals. *Fuel Process Technol* **67**(3):165-176 (2000).
43. Bryers RW. Fireside slagging, fouling, and high-temperature corrosion of heat-transfer surface due to impurities in steam-raising fuels. *Prog Energy Combust Sci* **22**(1):29-120 (1996).
44. Harb JN, Smith EE. Fireside corrosion in pc-fired boilers. *Prog Energy Combust Sci* **16**(3):169-190 (1990).
45. Shamanna S, Schobert HH. Fireside corrosion of selected alloys by ash recovered from coal-water slurry combustion, *Fuel Process Technol* **53**(1-3):133-156 (1997).
46. James DW, Krishnamoorthy G, Benson SA and Seames WS, Modelling trace element partitioning during coal combustion. *Fuel Process Technol* **126**:284-297 (2014).

47. Moser RE. Benefits of effective SO_3 removal in coal-fired power plants: beyond opacity control. In: *Power Plant Air Pollutant Control, Mega Symposium,* August 28-31, Baltimare, MD (2006).
48. Nielsen MT. On the relative importance of SO_2 oxidation to high dust SCR DeNOx units. In: *DOE/NETL 2003 Conference on Selective Catalytic Reduction (SRC) and Selective Non-Catalytic Reduction (SNCR) for NOx Control,* pp. 1-12 (2003).
49. Fleig D, Normann F, Andersson K, Johnsson F and Leckner B, The fate of sulphur during oxy-fuel combustion of lignite. *Energy Procedia* **1**(1):383-390 (2009).
50. Fleig D, Andersson K and Johnsson F, Influence of operating conditions on SO_3 formation during air and oxy-fuel combustion. *Ind Eng Chem Res* **51**(28):9483-9491 (2012).
51. Tan Y, Croiset E, Douglas MA and Thambimuthu KV, Combustion characteristics of coal in a mixture of oxygen and recycled flue gas. *Fuel* **85**(4):507-512 (2006).
52. Reid WT. External Corrosion and Deposits Boilers and Gas Turbines. (Elsevier, ed), New York (1971).
53. Svachula J, Alemany LJ, Ferlazzo N, Forzatti P and Tronconi E, Oxidation of SO_2 to SO_3 over honeycomb DeNoxing Catalysts. *Ind Eng Chem Res* **32**:826-834 (1993).
54. EPRI, *SO_3 Mitigation Guide* , EPRI Report TR-104424, Research Project 2250-03,Prepared by Radian Corporation, Austin, Texas. Principal investigators Peterson J, Jones AF. October (1994).
55. Shanthakumar S, Singh DN and Phadke RC, Flue gas conditioning for reducing suspended particulate matter from thermal power stations. *Prog Energy Combust Sci*. **34**(6):685-695 (2008).
56. Sjostrom S, Dillon M, Donnelly B, Bustard J, Filippelli G, Glesmann R *et al.,* Influence of SO_3 on mercury removal with activated carbon: Full-scale results. *Fuel Process Technol* **90**(11):1419-1423 (2009).
57. Hu Y, Yan J. Characterization of flue gas in oxy-coal combustion processes for CO_2 capture. *Appl Energy* **90**(1):113-121 (2012).
58. Boot-Handford ME, Abanades JC, Anthony EJ, Blunt MJ, Brandani S, Mac Dowell N *et al.,* Carbon capture and storage update. *Energy Environ Sci* **7**(1):130-189 (2014).
59. Kather A, Scheffknecht G. The oxycoal process with cryogenic oxygen supply. *Naturwissenschaften* **96**(9):993-1010 (2009).
60. Nakayama S, Noguchi Y, Kiga T, Miyamae S, Maeda U, Kawai M *et al.,* Pulverized coal combustion in O_2/CO_2 mixtures on a power plant for CO_2 recovery. *Energy Convers Manag* **33**(5-8):379-386 (1992).

61. Normann F, Andersson K, Leckner B and Johnsson F, Emission control of nitrogen oxides in the oxy-fuel process. *Prog Energy Combust Sci* **35**(5):385-397 (2009).
62. Molburg JC, Doctor RD, Brockmeier NF and Plasynski S, CO_2 capture from PC boilers with O_2-firing. In: *18th Annual International Pittsburgh Coal Conference,* December 4-7, Newcastle, New South Wales, Australia (2001).
63. *Review of CO_2-Capture Development Activities for Coal-Fired Power Generation Plants*, EPRI, Palo Alto, CA: 2007: 1012239.
64. Zanganeh KE, Shafeen A. A novel process integration, optimization and design approach for large-scale implementation of oxy-fired coal power plants with CO_2 capture. *Int J Greenh Gas Control* **1**(1):47-54 (2007).
65. Günther C, Weng M and Kather A, Restrictions and limitations for the design of a steam generator for a coal-fired oxyfuel power plant with circulating fluidised bed combustion. *Energy Procedia* **37**:1312-1321 (2013).
66. Kiga T, Takano S, Kimura N, Omata K, Okawa M, Mori T *et al.,* Characteristics of pulverized-coal combustion in the system of oxygen/recycled flue gas combustion. *Energy Convers Manag* **38**:S129-S134 (1997).
67. Dhungel B, Ellul C, Gibson JR and Fitzgerald FD, SO_3 Control in Oxyfuel Applications. In: *IEAGHG Special Workshop on Oxyfuel Combustion. London: IEA Greenhouse Gas R&D Programme* (2011).
68. Fleig D, Andersson K, Kühnemuth D, Normann F, Johnsson F and Leckner B. The sulphur mass balance in oxy-fuel combustion of lignite - an experimental study. In: *1st Oxyfuel Combustion Conference*, Cottbus, 8-11th September (2009). Available at: http://www.ieaghg.org/docs/oxyfuel/OCC1/Session%205_A/Cottbus%20Daniel%20Fleig.pdf [accessed 5 March 2017].
69. Duan L, Sun H, Zhao C, Zhou C. Zhou W and Chen X, Coal combustion characteristics on an oxy-fuel circulating fluidized bed combustor with warm flue gas recycle. *Fuel* **127**:47-51 (2014).
70. Durie RA, Matthews CJ and Smith MY, The catalytic formation of sulfur trioxide in fuel-rich propane-air flames. *Combust Flame* **15**(2):157-165 (1970).
71. Zachariah MR, Smith OI. Experimental and numerical studies of sulfur chemistry in $H_2/O_2/SO_2$ flames. *Combust Flame* **69**(2):125-139 (1987).
72. Miccio F, Löffler G, Wargadalam VJ and Winter F, The influence of SO_2 level and operating conditions on NO_x and N_2O emissions during fluidised bed combustion of coals. *Fuel* **80**(11):1555-1566 (2001).
73. Schäfer S, Born B. Hydrolysis of HCN as an important step in nitrogen oxide formation in fluidised combustion. Part II: heterogeneous reactions involving limestone. *Fuel* **81**(13):1641-1646 (2002).
74. Wendt JOL, Ekmann JM. Effect of fuel sulfur species on nitrogen oxide emissions from premixed flames. *Combust Flame* **25**:355-360 (1975).

75. Wendt JOL, Wootan EC and Corley TL, Postflame behavior of nitrogenous species in the presence of fuel sulfur I. Rich, moist CO/Ar/O_2 flames. *Combust Flame* **49**(1-3):261-274 (1983).
76. Corley TL, Wendt JOL. Postflame behavior of nitrogenous species in the presence of fuel sulfur II. Rich, CH_4/He/O_2 flames. *Combust Flame* **58**(2):141-152 (1984).
77. Glarborg P, Kubel D, Dam-Johansen K, Chiang HM and Bozzelli JW, Impact of SO_2 and NO on CO oxidation under post-flame conditions. *Int J Chem Kin* **28**(10):773-790 (1996).
78. Rasmussen CL, Glarborg P and Marshall P, Mechanisms of radical removal by SO_2. *Proc Combust Inst* **31**(1):339-347 (2007).
79. Giménez-López J, Martínez M, Millera A, Bilbao R and Alzueta MU, SO_2 effects on CO oxidation in a CO_2 atmosphere, characteristic of oxy-fuel conditions. *Combust Flame* **158**(1):48-56 (2011).
80. Jørgensen TL. Livbjerg H and Glarborg P, Homogeneous and heterogeneously catalyzed oxidation of SO_2. *Chem Eng Sci* **62**(16):4496-4499 (2007).
81. Burdett NA, Langdon WE and Squires RT, Rate of the coefficients for the reaction $SO_2 + O_2 \rightarrow SO_3 + O$ in the temperature range 900-1350 K. *J Inst Energy* **57**:373-376 (1984).
82. Mulcahy MFR, Steven JR, Ward JC and Williams DJ, Kinetics of interaction of oxygen atoms with sulfur oxides. *Symp (International) Combust* **12**(1):323-330 (1969).
83. Mulcahy MFR, Steven JR and Ward JC, The kinetics of reaction between oxygen atoms and sulfur dioxide: an investigation by electron spin resonance spectrometry. *J Phys Chem* **71**(7):2124-2131 (1967).
84. Yilmaz A, Hindiyarti L, Jensen AD, Glarborg P and Marshall P, Thermal dissociation of SO_3 at 1000-1400 K. *J Phys Chem A* **110**(21):6654-6659 (2006).
85. Merryman EL, Levy A. Enhanced SO_3 emissions from staged combustion. In: *Symp (International) Combust*. **17**(1):727-736 (1979).
86. Naidoo J, Goumri A and Marshall P, A kinetic study of the reaction of atomic oxygen with SO_2. *Proc Combust Inst* **30**(1):1219-1225 (2005).
87. Blitz MA, Hughes KJ and Pilling M, Determination of the high-pressure limiting rate coefficient and the enthalpy of reaction for OH + SO2. *J Phys Chem A* **107**(12):1971-1978 (2003).
88. Duan L, Duan Y, Sarbassov Y, Li Y and Anthony EJ, SO_3 formation under oxy-CFB combustion conditions. *Int J Greenh Gas Control* **43**:172-178 (2015).
89. Belo LP, Elliott LK, Stanger RJ, Spörl R, Shah KV, Maier J *et al*., High-Temperature conversion of SO_2 to SO_3: homogeneous experiments and catalytic effect of fly ash from air and oxy-fuel firing. *Energy Fuels* **28**:7243-7251 (2014).
90. Fleig D, Alzueta MU, Normann F, Abián M, Andersson K and Johnsson F, Measurement and modeling of sulfur trioxide formation in a flow reactor under post-flame conditions. *Combust Flame* **160**(6):1142-1151 (2013).

91. Wang X, Liu X, Li D, Zhang Y and Xu M, Effect of steam and sulfur dioxide on sulfur trioxide formation during oxy-fuel combustion. *Int J Greenh Gas Control* **43**:1-9 (2015).
92. Colorado State University. Chemical equilibrium calculation. Available at: http://navier.engr.colostate.edu/~dandy/code/code-4/index.html [accessed 15 September 2017].
93. Urbanek A, Trela M. Catalytic oxidation of sulfur dioxide. *Catal Rev Sci Eng* **21**:73-133 (1980).
94. Marier P, Dibbs HP. The catalytic conversion of SO_2 to SO_3 by fly ash and the capture of SO_2 and SO_3 by CaO and MgO. *Thermochim Acta* **8**(1-2):155-165 (1974).
95. Zhang X, Zhuang G, Chen J, Wang Y, Wang X, An Z *et al*., Heterogeneous reactions of sulfur dioxide on typical mineral particles. *J Phys Chem* **110**(25):12588-12596 (2006).
96. Tronconi E, Cavanna A, Orsenigo C and Forzatti P, Transient kinetics of SO_2 oxidation over SCR-DeNOx monolith catalysts. *Ind Eng Chem Res* **38**(7):2593-2598 (1999).
97. Dunn JP, Koppula PR, Stenger HG and Wachs IE, Oxidation of sulfur dioxide to sulfur trioxide over supported vanadia catalysts. *Appl Catal B Environ* **19**(2):103-117 (1998).
98. Thibault JD. Steward FR and Ruthven DM, The kinetics of absorption of SO_3 in calcium and magnesium oxides. *Can J Chem Eng* **60**(6):796-801 (1982).
99. Galloway BD, Sasmaz E and Padak B, Binding of SO_3 to fly ash components: CaO, MgO, Na_2O and K_2O. *Fuel* **145**:79-83 (2015).
100. Cao Y, Zhou H, Jiang W, Chen CW and Pan WP, Studies of the fate of sulfur trioxide in coal-fired utility boilers based on modified selected condensation methods. *Environ Sci Technol* **44**(9):3429-3434 (2010).
101. Chang CC. Infrared studies of SO_2 on γ-alumina. *J Catal* **53**(3):374-385 (1978).
102. Jaworowski RJ, Mack SS. Evaluation of methods for measurement of SO_3/H_2SO_4 in flue gas. *J Air Pollut Control Assoc* **29**(1):43-46 (1979).
103. Fleig D, Vainio E, Andersson K, Brink A, Johnsson F and Hupa M, Evaluation of SO_3 measurement techniques in air and oxy-fuel combustion. *Energy Fuels* **26**:5537-5549 (2012).
104. ASTM D3226. Method of test for sulfur oxides in flue gases (barium chloranilate controlled condensation method). Withdrawn from 1978. Available at: http://www.astm.org/DATABASE.CART/WITHDRAWN/D3226.htm [accessed 27 August 2017].
105. BS 1756-4:1977, Methods for sampling and analysis of flue gases. Miscellaneous analyses. Withdrawn from 01 February 2008. Available at: http://shop.bsigroup.com/en/ProductDetail/?pid=000000000000052803 [accessed 27 August 2017].

106. NCASI Southern Regional Center, Method 8a-Determination of sulfuric acid vapor or mist and sulfur dioxide emissions from kraft recovery furnaces; pp.1-87, (1996). Available at: https://www3.epa.gov/ttnemc01/ctm/ctm-013.pdf [accessed 19 November 2017].
107. Maddalone RF, Newton SF, Rhudy RG and Statnick RM, Laboratory and field evaluation of the controlled condensation system for SO_3 measurements in flue gas streams. *J Air Pollut Control Assoc* **29**(6):626-631 (1979).
108. Dellinger B, Grotecloss G, Fortune CR, Cheney JL and Homolya JB, Sulfur dioxide oxidation and plume formation at cement kilns. *Environ Sci Technol* **14**(10):1244-1249 (1980).
109. Cooper D. Optimization of a NaCl Adsorbent Tube Method for SO_3 Measurements in Combustion Flue Gases. Report B-1177; Institute för Vattenoch Luftvardsforskning (IVL): Göteburg, (1995).
110. Kelman FN. Direct method on determination of the sulfuric acid in solution with sulfuric gases and air. *Zavod Lab* **11**:1316-1318 (1952) (in Russian).
111. Vainio E, Fleig D, Brink A, Andersson K, Johnsson F and Hupa M, Experimental evaluation and field application of a salt method for SO_3 measurement in flue gases. *Energy Fuels* **27**:2767-2775 (2013).
112. Cooper D, Andersson C. Determination of SO_3 in flue gases using the NaCl method - a comparison with other techniques (Bestamning av SO_3 I rökgaser med NaCl-methoden – en jämförelse av olika metoder), Värmeforsk Report 616; (1994), (In Swedish).
113. Ibanez JG, Batten CF and Wentworth WE, Simultaneous determination of $SO_{3(g)}$ and $SO_{2(g)}$ in a flowing gas. *Ind Eng Chem Res* **47**(7):2449-2454 (2008).
114. Fateev A, Clausen S. Sulfur trioxide on-line measurement technique for power plants. In: IEAGHG Workshop. *Special Workshop on Oxyfuel Combustion*. London, 25-26 January (2011). Available at: http://orbit.dtu.dk/files/10145781/Fateev_SO3_workshop_London.pdf [accessed 01 October 2017].
115. Continuous Measurement Technologies for SO_3 and H_2SO_4 in Coal-Fired Power Plants, EPRI, Palo Alto, CA: 2004. 1009812.
116. Chamberlain S, Reeder T, Stimpson CK and Tree DR, A comparison of sulfur and chlorine gas species in pulverized-coal, air- and oxy-combustion. *Combust Flame* **160**(11):2529-2539 (2013).
117. Roy B, Chen L and Bhattacharya S, Nitrogen oxides, sulfur trioxide, and mercury emissions during oxy-fuel fluidized bed combustion of Victorian brown coal. *Environ Sci Technol* **48**(24):14844-14850 (2014).
118. Jackson PJ, Hilton DA and Buddery JH, Continuous measurement of sulphuric acid vapour in combustion gases using a portable automatic monitor. *J Inst Energy* **54**:124-135 (1981).
119. SO_3 Monitor. How much SO_3 do you generate? Available at: http://www.pentol.net/_pdf/so3monitor-EN.pdf [Accessed 7 September 2017].

120. Dennis JS, Hayhurst AN. The formation of SO_3 in a fluidized bed. *Combust Flame* **72**(3):241-258 (1988).
121. Verhoff FH, Banchero JT. Predicting dew points of flue gases. *Chem Eng Prog* **70**(8):71-72 (1974).
122. ZareNezhad B. New correlation predicts flue gas sulfuric acid dewpoints. *Oil Gas J* **107**(35):60-63 (2009).
123. Taylor HD. The condensation of sulphuric acid on cooled surfaces exposed to hot gases containing sulphur trioxide. *Trans Faraday Soc* **47**:1114-1120 (1951).
124. Stuart DD. Acid dewpoint temperature measurement and its use in estimating sulfur trioxide concentration. Available at: https://www.researchgate.net/profile/Derek_Stuart2/publication/265801421_Acid_dewpoint_temperature_measurement_and_its_use_in_estimating_sulfur_trioxide_concentration/links/59a0340c0f7e9b0fb8990820/Acid-dewpoint-temperature-measurement-and-its-use-in-estimating-sulfur-trioxide-concentration.pdf [accessed 05 November 2017].
125. Ahn J, Okerlund R, Fry A and Eddings EG, Sulfur trioxide formation during oxy-coal combustion. *Int J Greenh Gas Control* **5S**: S127-S135 (2011).
126. Fleig D, Andersson K, Normann F and Johnsson F, SO_3 formation under oxy fuel combustion conditions. *Ind Eng Chem Res* **50**(14):8505-8514 (2011).
127. Spörl R, Walker J, Belo L, Shah K, Stanger R, Maier J *et al.*, SO_3 emissions and removal by ash in coal-fired oxy-fuel combustion. *Energy Fuels* **28**(8):5296-5306 (2014).
128. Belo LP, Elliott LK, Stanger RJ,Spörl R, Shah KV, Maier J *et al*., Laboratory investigations on the differences in the homogeneous and catalytic conversions with fly ash of SO_2 to SO_3 from air and oxy-fuel PF combustion. In: *Impacts of Fuel Quality on Power Production*. 26-31st October, Snowbird, Utah (2014).
129. Zheng L, Furimsky E. Assessment of coal combustion in O_2+CO_2 by equilibrium calculations. *Fuel Process Technol* **81**(1):23-34 (2003).
130. Armitage JW, Cullis CF. Studies of the reaction between nitrogen dioxide and sulfur dioxide. *Combust Flame* **16**(2):125-130 (1971).
131. Wendt JOL, Sternling CV. Catalysis of SO_2 oxidation by nitrogen oxides. *Combust Flame* **21**(3):387-390 (1973).
132. Kühnemuth D, Normann F, Andersson K and Johnsson F, On the carbon monoxide formation in oxy-fuel combustion—Contribution by homogenous and heterogeneous reactions. *Int J Greenh Gas Control* **25**:33-41 (2014).
133. Seddighi S, Pallarès D, Normann F and Johnsson F, Carbon monoxide formation during oxy-fuel-fired fluidized-fed combustion. *Energy Fuels* **27**(4):2275-2282 (2013).
134. Glarborg P, Bentzen LLB. Chemical effects of a high CO_2 concentration in oxy-fuel combustion of methane. *Energy Fuels* **22**:291-296 (2007).
135. Bayless DJ, Jewmaidang J, Tanneer S and Birru R, Kinetics of low-temperature homogeneous SO_3 formation for use in flue gas conditioning for improved

electrostatic precipitator performance. In: *Proceedings of the Combustion Institute* **28**:2499-2505 (2000).
136. Hecht ES, Shaddix CR, Geier M, Molina A and Haynes BS, Effect of CO_2 and steam gasification reactions on the oxy-combustion of pulverized coal char. *Combust Flame* **159**(11):3437-3447 (2012).
137. Wine PH, Thompston RJ, Ravishankara AR, Semmes DH, Gump CA, Torabi A *et al*., Kinetics of the reaction OH + SO_2 + M → $HOSO_2$ + M. Temperature and pressure dependence in the falloff region. *J Phys Chem* **88**(10):2095-2104 (1984).
138. Hindiyarti L, Glarborg P and Marshall P. Reactions of SO_3 with the O/H radical pool under combustion conditions. *J Phys Chem A* **111**(19):3984-3991 (2007).
139. Flint D, Lindsay AW. Catalytic oxidation of sulphur dioxide on heated quartz surfaces. *Fuel* **30**:288 (1951).
140. Crumley PH, Fletcher AW. The formation of sulphur trioxide in flue gases. *J Inst Fuel* **29**:322-327 (1956).
141. Barret RE, Hummell JD and Reid WT, Formation of SO_3 in a noncatalytic combustor. *J Eng Power* **88**:165-172 (1966).
142. Couling D. Impact of oxyfuel operation on emissions and ash properties based on E.ON's 1MW CTF. In: *IEAGHG Special Workshop on Oxyfuel Combustion,* 25-26 January, London (2011).
143. Kenney JR, Clark MM, Levasseur AA and Kang SG, SO_3 emissions from a tangentially- fired pilot scale boiler operating under oxy-combustion conditions. In: *IEAGHG Special Workshop on Oxyfuel Combustion,* 25-26 January, London (2011).
144. Jurado N, Darabkhani HG, Anthony EJ and Oakey JE, Oxy-combustion studies into the co-firing of coal and biomass blends: effects on heat transfer, gas and ash compositions. *Energy Procedia* 63:440-452 (2014).
145. Spörl R, Belo L, Shah K, Stanger R, Giniyatullin R, Maier J *et al*., Mercury emissions and removal by ash in coal-fired oxy-fuel combustion. *Energy Fuels* **28**(1):123-135 (2014).
146. Spörl R, Maier J and Scheffknecht G, Experiences and Results of SO_3 measurements performed under oxy-coal fired conditions. In: *IEAGHG Special Workshop on Oxyfuel Combustion,* 25-26 January, London (2011).
147. Mönckert P, Dhungel B, Kull R and Maier J, Impact of combustion conditions on emission formation (SO_2, NO_x) and fly ash. In: *3rd meeting of the oxy-fuel combustion network.* Yokohama Symposia, Yokohama, Japan: IEA Greenhouse Gas R&D programme (2008).
148. Mitsui Y, Imada N, Kikkawa H and Katagawa A, Study of Hg and SO_3 behavior in flue gas of oxy-fuel combustion system. *Int J Greenh Gas Control* 5S:S143-S150 (2011).
149. Eddings EG, Wang L and Ahn J, Bench-scale fluid bed experiments of SO_2/SO_3 formation and sulfur capture in N_2/O_2 and SO_2/O_2 environments. In: *IEAGHG*

Special Workshop on SO_2/SO_3/Hg/Corrosion Issues in Oxycoal Combustion Boiler and Flue Gas Processing Units, 25-26 January, London (2011).
150. Spörl R, Maier J, Belo L, Shah K, Stanger R, Wall T *et al*., Mercury and SO_3 emissions in oxy-fuel combustion. In: *Energy Procedia* **63**:386-402 (2014).
151. Davis C. Impact of oxyfuel operation on corrosion in coal fired boilers based on experience with E.ON's 1MWth Combustion test facility. In: *IEAGHG Special Workshop on Oxyfuel Combustion,* 25-26 January, London (2011).
152. Stanger R, Belo L, Ting T, Spero C and Wall T, Mercury and SO_3 measurements on the fabric filter at the Callide Oxy-fuel Project during air and oxy-fuel firing transitions. *Int J Greenh Gas Control* **47**:221-232 (2016).
153. Glarborg P, Alzueta MU, Dam-Johansen K and Miller JA. Kinetic modeling of hydrocarbon/nitric oxide interactions in a flow reactor. *Combust Flame* **115**(1-2):1-27 (1998).
154. Schneider DR, Bogdan Z. Modelling of SO_3 formation in the flame of a heavy-oil fired furnace. *Chem Biochem Eng Q* **17**(3):175-181 (2003).